

1  
2  
3 **Biological Cybernetics manuscript No.**  
4 (will be inserted by the editor)  
5  
6  
7  
8  
9

10 Giancarlo La Camera · Michele Giugliano · Walter Senn · Stefano Fusi

# 11 **The response of cortical neurons to *in vivo*-like input current: theory** 12 **and experiment**

## 13 **I. Noisy inputs with stationary statistics**

14  
15  
16 Received: date / Revised: date  
17  
18  
19

20  
21  
22  
23 **Abstract** The study of several aspects of the collective dy-  
24 namics of interacting neurons can be highly simplified if one  
25 assumes that the statistics of the synaptic input is the same  
26 for a large population of similarly behaving neurons (mean  
27 field approach). In particular, under such an assumption, it is  
28 possible to determine and study all the equilibrium points of  
29 the network dynamics when the neuronal response to noisy,  
30 *in vivo*-like, synaptic currents is known. The response func-  
31 tion can be computed analytically for simple integrate-and-  
32 fire neuron models and it can be measured directly in ex-  
33 periments *in vitro*. Here we review theoretical and experi-  
34 mental results about the neural response to noisy inputs with  
35 stationary statistics. These response functions are important  
36 to characterize the collective neural dynamics that are pro-  
37 posed to be the neural substrate of working memory, deci-  
38 sion making and other cognitive functions. Applications to  
39 the case of time-varying inputs are reviewed in a compan-  
40 ion paper (Giugliano et al 2008). We conclude that modified

41  
42 G. La Camera is supported by the Intramural Research Program  
43 of the National Institute of Mental Health. M. Giugliano is sup-  
44 ported by the European Commission (FACETS Project FP6-2004-  
45 IST-FETPI-015879, EUSynapse Project LSHM-CT-2005-019055). W.  
46 Senn is supported by the Swiss National Science Foundation, grant No  
47 3152A0-105966. S. Fusi is supported by the Swiss National Science  
48 Foundation, grant PP00A-106556. The views expressed in this article  
49 do not necessarily represent the views of the NIMH, NIH, or the United  
50 States Government.

51 G. La Camera  
52 Laboratory of Neuropsychology, National Institute of Mental Health,  
53 National Institutes of Health, 49 Convent Dr, Rm 1B80, Bethesda, MD  
54 20892, USA. Tel.: +1-402-9759, Fax: +1-402-0046  
55 E-mail: lacamerag@gmail.com

56 M. Giugliano  
57 Laboratory of Neural Microcircuitry, Ecole Polytechnique Fédérale de  
58 Lausanne, Switzerland and Center for Theoretical Neurobiology, Uni-  
59 versity of Antwerp, Belgium

60 W. Senn  
61 Institute of Physiology, University of Bern, Switzerland

62 S. Fusi  
63 Center for Theoretical Neuroscience, Columbia University, New York,  
64 USA and Institute for Neuroinformatics, UNI/ETH Zurich, Switzer-  
65 land

integrate-and-fire neuron models are good enough to repro-  
duce faithfully many of the relevant dynamical aspects of the  
neuronal response measured in experiments on real neurons  
*in vitro*.

---

## 1 Introduction

Biological networks of neural cells are extremely compli-  
cated dynamical systems which comprise a large number of  
very diverse elements. Even within a single cortical column,  
where the neurons are known to have similar response prop-  
erties to external stimuli, the number of neurons can be as  
large as  $10^5$ , and the synaptic connections are of the order  
of  $10^9$  (Braitenberg and Schüz 1991). A study of detailed  
dynamical models of such networks is a difficult task. An  
alternative approach is suggested by the analogy between  
the neural circuits and physical systems like the spin glasses  
in which the number of interacting elements is huge and  
the long range interactions allow for important simplifica-  
tions (Mezard et al 1987). The dynamics of every element,  
the spin, are driven by the field generated by thousands of  
other spins. If all spins have similar dynamical properties  
and the interactions have the same statistical properties, then  
the fields felt by different spins are approximately the same.  
Analogously, the dynamics of a large population of interact-  
ing neurons could be greatly simplified if we focus on the  
statistical properties of the total synaptic currents. Such an  
approach is named population density approach or mean-  
field theory (Knight 1972a,b; Amit and Tsodyks 1991a,b;  
Treves 1993; Abbott and van Vreeswijk 1993; Amit and  
Brunel 1997b; Fusi and Mattia 1999; Brunel and Hakim  
1999; Gerstner 2000; Nykamp and Tranchina 2000), as the  
fields acting on different spins, or the total synaptic current  
to different neurons, are replaced by their mean value across  
a population of different interacting elements that behave in  
a similar way. In earlier efforts (Knight 1972a,b), only the  
mean current would be taken into account. More recently,  
mean field theory has been extended to include both the aver-  
age input current and the amplitude of its fluctuations (Amit

and Tsodyks 1991a,b; Abbott and van Vreeswijk 1993; Amit and Brunel 1997b).

Once we know the average input current, we need one more element to characterize the dynamics of recurrent neural circuits. We need to know how the total somatic current is transformed into trains of spikes, that in turn generate a synaptic current in the connected neurons. If we have this element, not only can we characterize the average firing rate of a population, but we can also analyze the dynamical behavior of circuits in which populations of neurons generate inputs to themselves. This is fundamentally important to study the attractor dynamics of recurrent neural circuits and their states of persistent activity (Amit and Tsodyks 1991a,b; Amit and Brunel 1997b; Wang 1999), i.e., attractor states with many potential applications ranging from working memory (Amit 1995; Wang 2001; Brunel and Wang 2001) to decision making (Rolls and Deco 2001; Wang 2002; Wong and Wang 2006) and flexible sensorimotor mapping (Fusi et al 2007). The transduction function which transforms the somatic current into a train of spikes (named *response function* in this article) provides a compact characterization of the single neuron properties that are relevant to the collective behavior of large networks of similar cells. If the response function is known, mean field theory allows us to study systematically the behavior of large connected networks of spiking neurons (e.g., Amit and Brunel (1997b); Brunel and Hakim (1999); Brunel (2000a,b); Mattia and Del Giudice (2002); Fourcaud and Brunel (2002); Del Giudice et al (2003); Renart et al (2003); Curti et al (2004); Richardson (2007); Moreno-Bote et al (2008)). It is then valuable to obtain a theoretical and experimental characterization of the response function of cortical neurons, which depends on the specific type of cell under consideration. One possibility is to build a model, inject a typical current into a simulated neuron, and observe its response. On the other hand, for simple enough model neurons, a theoretical response function can be determined analytically, facilitating the applicability of the theory and the comparison with the experimental data. This has been done for several models in the class of integrate-and-fire (IF) neurons (e.g., Fourcaud and Brunel (2002); Fourcaud-Trocmé et al (2003); Renart et al (2003); La Camera et al (2004a); Moreno-Bote and Parga (2005); Richardson (2007)). Experimentally, it is possible to measure neuronal response functions by injecting a real neuron with an appropriate range of input currents and measuring the neuron's response (Rauch et al 2003; Giugliano et al 2004; La Camera et al 2006; Arsiero et al 2007).

Beside the theoretical importance of the response function to study network behavior, its experimental characterization can be used i) to classify neurons (e.g., quantify their functional similarity); ii) to establish how well the simple models of spiking neurons used in theoretical studies represent the behavior of real neurons; iii) to modify simple model neurons so as to improve their ability to predict the behavior of real neurons, sometimes simply by using effective parameters (i.e., those derived from fitting the theoretical response functions to the experimental ones). Often these

parameters are different from those directly estimated with more traditional techniques.

In this article, we review the theoretical and experimental characterization of the response function of cortical neurons in the case of stationary statistics of the somatic current. In particular, we review the results related to the stationary response of the neuron on a time-scale of seconds, following a phase of fast adaptation (hundreds of milliseconds) for the pyramidal cells. The extension to the case of time-varying statistics and to the response on longer time-scales is addressed in a companion article (Giugliano et al 2008). This article is organized as follows. In Sec. 2, the relevant characteristics of cortical spike trains are summarized. In Sec. 3, the theory of the response function of cortical neurons is presented in the context of mean field theory. In Sec. 4, some of the applications of the theory are reviewed. In Sec. 5, we collate the various experimental characterizations of the response function of pyramidal and fast spiking neurons obtained in different areas of the rat neocortex, and compare the theory to the data. We finally discuss some of the advantages and some of the shortcomings of using the simplified spiking models and the approach reviewed in this article.

---

## 2 Cortical spike trains

To develop a theory of the response of cortical neurons, we must have an adequate understanding of the typical neuronal spike patterns as observed *in vivo*. Recording neural activity from the cerebral cortex of anesthetized and awake animals has shown that such activity is highly variable. In particular, it is observed i) a large variability in the inter-spike intervals (ISIs) of the same neuron during spontaneous as well as stimulus-driven activity (e.g., Noda and Adey (1970); Holt et al (1996); Shinomoto et al (2003)); ii) a large trial-by-trial variability of the spike count of the same neuron in response to repeated, identical stimulation, which grows proportionally with the average number of spikes (e.g., Gershon et al (1998); Lee et al (1998); Oram et al (1999); Wiener et al (2001)). Intracellular recordings of neural activity in the intact brain have also shown the presence of a large variability at the level of the subthreshold membrane potential, and have shed some light on the nature of this variability. In Fig. 1 is shown the intracellular recording of the membrane voltage of two pyramidal neurons from the visual cortex of adult cats performed by Holt et al (1996): one from a slice in response to a DC current injection (left); one from an intact animal under DC current injection (middle); and one under visual stimulation (right). Note how a constant current stimulation *in vitro* elicits a fairly regular spike train (left), whereas the same current injected *in vivo* (middle) elicits an irregular spike train very similar to that obtained in response to a visual stimulation (right).

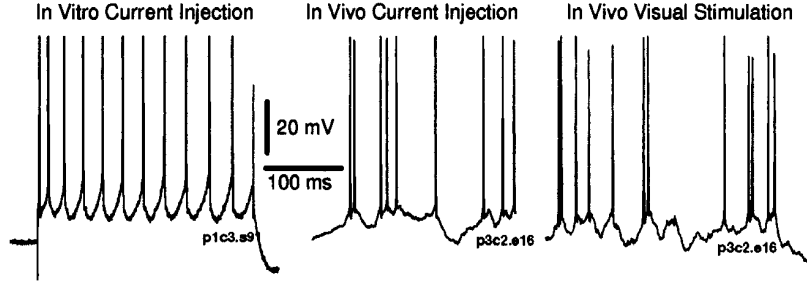


**Fig. 1 Neural activity *in vitro* and *in vivo*.** Comparison of primary visual cortex cells from adult cats in slice and *in vivo*. Sample traces from 2 pyramidal neurons, one from a slice (left) and one from an intact animal on the boundary layers II and III that was stimulated by current injection (middle) and by a bar moving along the receptive field (right). Note the lack of a large difference in spiking variability in response to current and visual stimulation in the intact animal. Used and modified with permission from Holt et al (1996). Copyright © 1996 by the American Physiological Society.

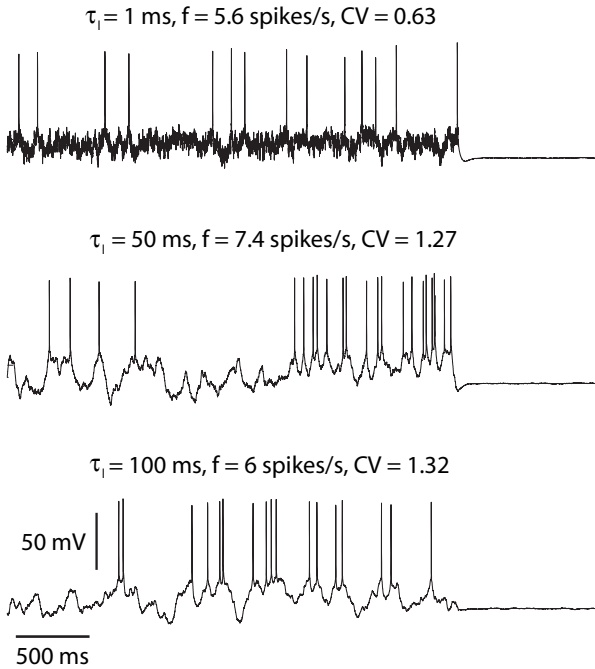


**Fig. 2 Neural activity *in vitro* in response to *in vivo*-like input current.** Three intracellular somatic recordings performed *in vitro* from one pyramidal neuron from layer 5 of the somatosensory cortex of a juvenile rat are shown. These somatic recordings were obtained in the whole cell configuration under current clamp in response to current injection modelled after Eq. 1 (Ornstein-Uhlenbeck process). Mean ( $m_I$ ), variance ( $s_I^2$ ), and time correlation length (reported at the top of each panel as  $\tau_I$ ; see Eq. 1) of the input current were adjusted so as to have roughly the same output spike rates ( $f$ ) but different coefficients of variability (CV). See Rauch et al (2003) for details.

## 2.1 Recreating *in vivo*-like activity *in vitro*

Whatever makes the neural activity irregular in an intact brain is not present in the DC stimulation *in vitro*, the traditional probe of the physiological and cellular properties of cortical neurons (e.g., Connors et al (1982); McCormick

et al (1985)). One explanation for this phenomenon lies in the fact that a cortical neuron is constantly bombarded by hundreds of seemingly erratic inputs. Indeed, whatever variability is contributed by the mechanism of action potential generation (Gutkin and Ermentrout 1997), this is present in both the cases illustrated in the left and middle plots of Fig. 1, and thus it can not account for the striking difference in variability. This explanation is confirmed by the fact that the irregular activity shown in Fig. 1 can be recreated *in vitro* in response to fluctuating, *in vivo*-like current, as shown in Fig. 2.

The current injected into the neuron shown in Fig. 2 was modeled after an Ornstein-Uhlenbeck process (see e.g. (Cox and Miller 1965; Gardiner 1985)),

$$dI = -\frac{I}{\tau_I}dt + \frac{m_I}{\tau_I}dt + s_I\sqrt{\frac{2dt}{\tau_I}}\xi_t. \quad (1)$$

The quantity  $\xi_t$  in Eq. 1 is a Gauss-distributed variable with zero mean and unitary variance, with the additional property that  $\langle \xi_t \xi_{t'} \rangle = \delta(t - t')$ , where  $\delta$  is Dirac's delta function and  $\langle \cdot \rangle$  means average over time. The process  $\xi_t$  is often referred to as 'white noise' in the literature. This condition defines a delta-correlated process and means that two values of  $\xi_t$  at different times  $t$  and  $t'$  are completely independent of each other.  $I$  is Gauss-distributed at any time  $t$ , and after a transient of the order of the  $\tau_I$  (the 'correlation length'), converges to a process with mean value  $m_I$  and standard deviation  $s_I$ . With the use of current Eq. 1 it is possible to generate *in vivo*-like spike trains *in vitro* with different firing rates, and different variability at parity of firing rate, as shown in Fig. 2. As we will show in Sec. 5, by tuning the values of parameters  $m_I$  and  $s_I$  a whole range of *in vivo*-like spike trains can be induced in the stimulated neuron.

## 2.2 Model reduction of cortical spike trains

In this article, we adopt the view that i) a spike train is completely defined by the sequence of its ISIs, and ii) a good model reduction of cortical neurons is one that predicts well its spike trains under conditions as close as possible to the

one experimentally measured in the intact brain. How well, it depends on the underlying problem that a network of spiking neurons is called upon to describe, and different time resolutions have been found to be optimal in different systems (see Victor (2005) for a review). Some authors have assumed as a criterion that a large percentage of ISIs be predicted within  $\pm 2$  ms (Jolivet et al 2004, 2006, 2008). We take a different approach and demand that the model neuron reproduces well the first and second order statistics of spike trains in response to *in vivo*-like current. A justification for this criterion is that a level of detail at the millisecond scale is not necessary for studying patterns of activity that do not vary much on time-scales of seconds (Sec. 3.1).

We will characterize a spike train by its firing rate (spike count in an interval divided by that interval's duration) and by its coefficient of variability, defined as the ratio of the standard deviation to the mean of the ISIs. For stationary spike trains, the firing rate quantifies also the average ISI, and the coefficient of variability and firing rate together quantify the variability of the ISIs. For non-stationary spike trains other measures of variability have been devised and should be used instead (Holt et al (1996); Shinomoto et al (2003); Kostal et al (2007); see Gabbiani and Koch (1998) for a primer on spike train analysis).

### 2.3 Stationarity of the statistics of the noisy input current

After a transient  $\sim \tau_I$ , the current  $I$  of Eq. 1 is auto-correlated over a time of order  $\tau_I$  (its autocorrelation function is  $\rho(t, t') = s_I^2 e^{-|t-t'|/\tau_I}$ , see e.g. Cox and Miller (1965)), and for very short  $\tau_I$  approaches a white noise process. Even for finite  $\tau_I$ , however, and despite being highly fluctuating in time,  $I$  is a stationary process in the statistical sense, since the statistics of the current are completely characterized by the three parameters  $m_I$ ,  $s_I$  and  $\tau_I$ , which are constant. In this sense, the highly variable spike trains obtained in response to such a current, shown in Fig. 2, are also stationary. Indeed, under rather general conditions, the input current Eq. 1 can be generated at the soma of a target neuron by linear summation of the post-synaptic potentials (PSPs) arising from many spike trains that are in turn obtained in response to the same type of current as Eq. 1.

The parameters  $m_I$ ,  $s_I$  and  $\tau_I$  represent, ideally, the most important component of the presynaptic contributions to the neuron under investigation. We shall link these parameters to presynaptic parameters in a later section (Sec. 3.2). Non-stationarity could arise from a time-dependence of any of these parameters. In this manuscript, we will be dealing with spike trains that are stationary in the sense defined above.

Having defined the scale at which we wish to characterize cortical spike trains, we move to the characterization of the input-output relationship at the corresponding level of description, i.e., the response function.

## 3 Theoretical analysis of the response of cortical neurons

The response function characterizes the response of a neuron to its somatic input current and thus plays an essential role in the dynamics of neural circuits. In the simplified scenario we are going to assume in the following, the average somatic current and the amplitude of its fluctuations are the only ingredients considered effective in driving the response (for more complex scenarios, taking e.g. into account the auto- and cross-correlations of input spike trains, see e.g. Sakai et al (1999); Svirsakis and Rinzel (2000); Salinas and Sejnowski (2002); Moreno et al (2002); Doiron et al (2004); Lerchner et al (2006); Moreno-Bote et al (2008)). Thus, we shall define the response function as the output firing rate as a function of the mean and variance of the input current. The response function plays a central role in the mean field theory of networks of spiking neurons (Knight 1972a,b; Amit and Tsodyks 1991a,b; Abbott and van Vreeswijk 1993; Amit and Brunel 1997b; Brunel and Sergi 1998; Fusi and Mattia 1999; Brunel and Hakim 1999; Brunel 2000a,b; Nykamp and Tranchina 2000; Fourcaud and Brunel 2002; Moreno et al 2002; Mattia and Del Giudice 2002; Del Giudice et al 2003; Lindner et al 2002; Renart et al 2003; Richardson 2004; Moreno-Bote and Parga 2004; Gigante et al 2007a; Richardson 2007; Moreno-Bote et al 2008). We provide a brief introduction to this theory in the next subsection. For a detailed mathematical exposition of the theory, the reader is referred e.g. to Abbott and van Vreeswijk (1993); Fusi and Mattia (1999); Brunel and Hakim (1999); Fourcaud and Brunel (2002); Moreno-Bote and Parga (2005) and Richardson (2007).

### 3.1 Neuronal mean field approach

Consider the neural circuits depicted in Fig. 3. Starting from a large network of interacting neurons (Fig. 3A), we group together those neurons that presumably have a similar behavior in a *statistical sense* (for example they fire at the same average rate). In this example, we consider two populations of cells: pyramidal neurons, schematically drawn in black, and gabaergic neurons, in gray. Two pyramidal neurons are labelled in Fig. 3B as “1” and “2”; they receive direct synaptic input from other neurons in the same population (red), and from the cells of the population of gabaergic neurons (blue), which in turn produce the typical noisy input currents as shown in figure (“current into the soma”). Different pyramidal neurons belonging to the same population will in general be driven by different somatic inputs, either because the pre-synaptic cells are different, or because the function that transforms the pre-synaptic spikes into a somatic current are different. However, the statistical properties of the somatic currents might be the same across different neurons of the same population. In the example of Fig. 3B, the specific realizations of the noisy somatic currents generated by the pyramidal neurons are clearly different. Nevertheless,

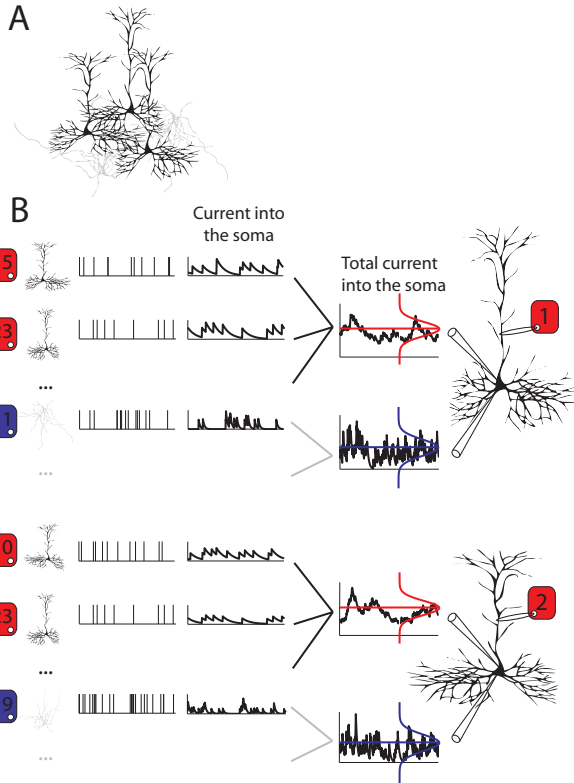


**Fig. 3 Mean field theory for neural circuits.** *A*: Two distinct populations of different types of neurons: pyramidal (black) and gabaergic cells (gray). Each population is made of different neurons that are tentatively grouped together due to the similarities in the statistics of the synaptic input and their response properties. *B*: Two cells (1 and 2, on the right) from the population of pyramidal neurons. The other pyramidal neurons (in red labels) and the gabaergic neurons (blue labels) that are connected (left) to the two cells shown on the right generate an excitatory and an inhibitory somatic current. If the statistics of the input currents to all pyramidal neurons is similar – same mean (red and blue lines) and average amplitude of the fluctuations (red and blue distributions) – then all the pyramidal neurons within the same population behave in a similar way and they can be replaced by a single representative neuron (e.g., neuron 1).

the average (the red line) and the variance (red bell-shaped curve) are approximately the same. Similarly, the mean and the variance of the inhibitory input (in blue) are also approximately the same. This means that if we replace the actual somatic inputs with one having the same mean average and variance across all neurons of the same population, we may not make a large mistake. This is the basic approximation of mean field theory: instead of considering the specific somatic input driving every individual neuron, we make the assumption that the same fluctuating input drives all the neurons. If all neurons react in the same way to the input, then it is unnecessary to study a large number of neurons, as they would all behave in the same way (in a statistical sense) under the mean field assumption. Hence, an entire popula-

tion can be replaced by a single representative neuron which is driven by the mean field. If we know how each neuron transforms the somatic current into a train of spikes (their response function), we then can fully characterize the population dynamics.

This approach has been named “extended mean field theory” by Amit and collaborators (Amit and Tsodyks 1991a,b; Amit and Brunel 1997b) because it takes into account the fluctuations of the input current. It is a stratagem that allows us to reduce a population of similar neurons to the study of a single representative neuron while, at the same time, taking into consideration non negligible fluctuations. It is important to include the fluctuations in the mean field approach not only because they are observed in real neural circuits, but also because they play an important role in working regimes similar to those observed *in vivo* (Troyer and Miller 1997; Fusi and Mattia 1999). When neurons are driven by fluctuations, the generated spike trains are highly irregular (Fig. 2). Moreover, the neurons are active also when driven by a mean current that is below the *rheobase* (i.e., the minimal non-noisy current needed to generate an action potential). As we will show in more detail in Sec. 4, this allows for the existence of stable states that have properties similar to those of the spontaneous activity observed *in vivo* (Amit and Brunel 1997b).

The response of a population of neurons can be stationary, quasi-stationary or time-dependent. By quasi-stationary, we mean slowly changing with time with respect to the relevant time-scale of the neural dynamics, which could be the membrane time constant in the case of single neurons, or the transient response time of a population of neurons considered as a unitary entity (Knight 1972a). In the quasi-stationary case, the statistics of the input current produced at the soma of each neuron, and the resulting spike trains produced by the same neuron, have quasi-stationary properties (typically, mean, variance and autocorrelation), and can be self-consistently described in the mean field approach outlined above. The same approach can be extended to the case of time-varying statistics of the input current, usually with *ad hoc* modifications customized to work for the relevant time-scale under consideration. Some of these extensions are reviewed in the companion paper (Giugliano et al 2008), whereas in this article we consider the response of cortical neurons in a regime of stationary or quasi-stationary activity. In the next subsections, we consider its quantitative development in the framework of networks of IF neurons.

### 3.2 The statistics of the somatic current for random uncorrelated inputs

Assume that a neuron receives inputs from  $N_e$  excitatory and  $N_i$  inhibitory neurons through synaptic contacts of strength  $J_{e,i}$  (in units of current), each neuron emitting independent and irregular spike trains with firing rate  $\nu_{e,i}$ , with each spike contributing an exponentially shaped PSP with a decay time constant of  $\tau_{e,i}$ , i.e.  $\propto e^{-t/\tau_{e,i}}$ . For independent spike trains,

the mean and the variance of the stochastic process,  $I$ , deriving from the summation of the PSPs emitted by the presynaptic neurons of the same type  $k \in \{e, i\}$ , are given by

$$m_k = N_k J_k v_k \tau_k, \quad s_k^2 = 0.5 N_k J_k^2 v_k \tau_k. \quad (2)$$

(A slight modification of the second of these equations is required if the synaptic weights are not identical but are drawn from a probability distribution (Amit and Brunel 1997b; Curti et al 2004)). We assume that a large number of small amplitude PSPs are required to reach the threshold. If this assumption is sufficient for a diffusion approximation to hold (Richardson and Gerstner 2005),  $I$  can be approximated by the algebraic sum of two OU component processes each evolving according to Eq. 1, with  $m_k, s_k$  given by Eq. 2 and  $k \in \{e, i\}$ . If  $\tau_e = \tau_i \equiv \tau_I$ , the two components can be merged in the single equation (1) with  $m_I = m_e - m_i, s_I^2 = s_e^2 + s_i^2$  (Amit and Brunel 1997b).

### 3.3 The integrate-and-fire neuron

The characterization of the input current Eq. 1 requires only a i) model for the PSPs, ii) the characterization of the spike trains as independent stochastic processes, and iii) the conditions for the diffusion approximation to be valid. To characterize the output spike train in response to a current of type Eq. 1, a model neuron must be specified. We are interested in the firing rate and variability of the output spike train. This can be calculated in analytical terms only if the model neuron is simple enough, for example in the case of IF neurons. A single-compartment IF neuron (Stein 1965; Knight 1972a; Tuckwell 1988) is completely characterized by its membrane potential at the soma  $V$ , i.e., electro-tonic compactness of the soma is assumed with no role for dendritic nonlinearities ('point-neuron' approximation). The membrane potential integrates its inputs in a linear fashion. When  $V$  reaches a threshold  $\theta$ , a spike is said to be emitted and the neuron is clamped to a reset potential  $V_r$  for a refractory time  $\tau_r$  during which it is not sensitive to presynaptic or electrical stimulation. IF neurons come in a large variety and most of the material covered in this article applies to most types, see e.g. La Camera et al (2004a). In the following, we shall limit ourselves to the leaky IF (LIF) neuron driven by an input current  $I$ :

$$\frac{dV}{dt} = -\frac{V - V_{rest}}{\tau} + \frac{I}{C}, \quad (3)$$

where  $V_{rest}$  is the membrane resting potential,  $C$  is the membrane capacitance, and  $\tau = RC$ , where  $R$  is the membrane resistance. To emulate the noisy input current targeting neurons *in vivo*, the current  $I$  is modeled as a stochastic process,  $I(t) = \sum_{k \in \{e, i\}} \sum_{t > t_{j,k}} s(t - t_{j,k})$ , where  $s(t)$  is the PSP (here  $\propto e^{-t/\tau_{e,i}}$  for consistency with Sec. 3.2), and  $\{t_{j,k}\}$  are the presynaptic spikes' arrival times from excitatory ( $k = e$ ) and inhibitory ( $k = i$ ) neurons respectively, both assumed to be exponentially distributed (Poisson spike trains; this model is usually credited to Stein (1965)). In the diffusion approximation (Lánský and Sato 1999; Richardson and Gerstner

2005) – which, roughly speaking, holds when a large number of small amplitude PSPs are required to reach the threshold – and for unitary PSPs (i.e., in the limit  $\tau_{e,i} \rightarrow 0$ , which transforms the PSPs in delta functions), the subthreshold dynamics of the membrane potential obeys the stochastic differential equation of the OU process,

$$dV = -\frac{V - V_{rest}}{\tau} dt + \mu dt + \sigma \xi_t \sqrt{dt}, \quad (4)$$

where

$$\mu = m_I/C, \quad \sigma = \sqrt{2\tau'} s_I/C \quad (5)$$

are the average and standard deviation in unit time of the membrane voltage, and  $\xi_t$  is a Gaussian process with flat spectrum and unitary variance as in Eq. 1.  $m_I$  and  $s_I^2$  are the average and the variance of the synaptic input current, and  $\sqrt{2\tau'}$  is a factor to preserve units ( $\tau' = 1$  ms, see e.g. Rauch et al (2003)). Under the conditions specified in Sec. 3.2,  $m_I$  and  $s_I^2$  are given by

$$m_I = N_e J_e v_e - N_i J_i v_i, \quad s_I^2 = N_e J_e^2 v_e + N_i J_i^2 v_i. \quad (6)$$

Note that here, unlike Eq. 2, the synaptic time constants do not appear because we have performed the limit  $\tau_{e,i} \rightarrow 0$ .

### 3.4 The response function of integrate-and-fire neurons

The response function of the LIF neuron Eq. 4 is (Capocelli and Ricciardi 1971; Amit and Tsodyks 1991a; Amit and Brunel 1997b)

$$f = \Phi(\mu, \sigma; \tau) \equiv \left[ \tau_r + \tau \int_{\hat{V}_r}^{\hat{\theta}} \sqrt{\pi} e^{-u^2} (1 + \text{erf}(u)) du \right]^{-1}, \quad (7)$$

where the ‘‘hat’’ operation applied to  $\theta$  and  $V_r$  is defined by  $\hat{z} \equiv (z - \mu\tau)/\sigma\sqrt{\tau}$ , or  $\hat{z} = (Cz - m_I\tau)/s_I\sqrt{2\tau'\tau}$  upon use of Eqs. 5 (Rauch et al 2003). To derive Eq. 7, the following boundary conditions must be imposed on Eq. 4: the process  $V \in ]-\infty, \theta[$  is absorbed upon hitting the threshold  $\theta$ , and re-enters its allowed domain from  $V_r$  after a refractory period  $\tau_r$  (see, e.g., Fusi and Mattia (1999)). These boundary conditions formalize the emission of an action potential in this model and are by far the most commonly used with IF neurons. However, it must be noted that different spike generation mechanisms may produce a different neuronal response to fluctuating input (Fourcaud-Trocmé et al 2003; Fourcaud-Trocmé and Brunel 2005; Richardson 2007). Eq. 7 is plotted in Fig. 4 for different values of  $s_I$ . Its analytical form holds exactly for a white noise input, but only approximately for an input given by the OU process Eq. 1 with a small time constant  $\tau_I$ . A better approximation than Eq. 7 for a small  $\tau_I$  has been given by Brunel and Sergi (1998) and it amounts to an effective modification of the threshold  $\hat{\theta}$  and reset potential  $\hat{V}_r$  (see also Fourcaud and Brunel (2002)). In the absence of input fluctuations (e.g., for  $s_I \rightarrow 0$ ), Eq. 7 reduces to the well-known response function of the leaky integrator (e.g., Tuckwell (1988); Burkitt (2006)),

$$\Phi(m_I) = \left( \tau_r + \tau \ln \frac{m_I\tau - CV_r}{m_I\tau - C\theta} \right)^{-1} \Xi(m_I\tau - C\theta), \quad (8)$$

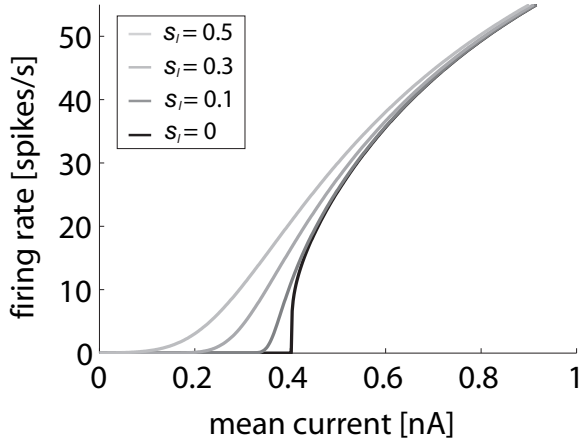


**Fig. 4 Stationary response function of the LIF neuron.** Response function of the white-noise driven LIF neuron, Eq. 7. Each curve is the  $f$ - $I$  curve for a constant value of the standard deviation of the input current,  $s_I$  (nA). The rightmost curve is Eq. 7 in the limit  $s_I \rightarrow 0$ , i.e., Eq. 8. Note the logarithmic singularity at rheobase  $m_I = C\theta/\tau \approx 0.4$  nA, i.e., the minimal constant current required for an action potential to be emitted in the absence of input fluctuations. Neuron parameters:  $\tau = 26.3$  ms,  $\tau_r = 9.4$  ms,  $C = 0.53$  nF,  $\theta = 20$  mV,  $V_r = 9.9$  mV,  $V_{rest} = 0$  mV.

where  $\Xi(x) = 1$  if  $x > 0$ , and zero otherwise.  $C\theta/\tau$  is the rheobase current for this model neuron (i.e., the minimal input current required for an action potential to be emitted in the absence of input fluctuations, see, e.g., Connors et al (1982)). Note that the LIF neuron is not quiescent below rheobase in the presence of input fluctuations, due to the occasional input fluctuation able to drive the membrane potential across the threshold. In the literature, this activity regime is called ‘noisy-dominated’, ‘fluctuation-dominated’, or simply ‘subthreshold’ regime. In the absence of fluctuations, no spikes can be emitted for inputs below the rheobase. The simplest response function used in the literature to model this phenomenon is threshold-linear around the rheobase. Instead, Eq. 8 has a singularity at rheobase, specifically, its derivative with respect to  $m_I$  diverges as  $m_I \rightarrow C\theta/\tau$ . We will come back to this point when discussing firing rate adaptation in Sec. 3.6.

### 3.5 The response function in the presence of reversal potentials

The theory presented so far can be extended to the so-called conductance-based IF neuron, or, more correctly, to the IF neuron with reversal potentials. This model brings IF neurons closer to biology by taking into account that the PSPs are voltage-dependent, i.e., depend on the current state of the neuronal membrane. Formally, the input current  $I$  in Eq. 3 depends on the membrane potential as  $I = \sum_x \bar{g}_x (V_x - V)$ , where  $x$  identifies the type of receptor mediating the cur-

rent (e.g., AMPA, NMDA, etc.),  $\bar{g}_x$  is its peak conductance, and  $V_x$  its reversal potential. We shall limit ourselves the LIF neurons with only two classes of conductances, excitatory and inhibitory, and will refer to it as the conductance-based LIF neuron. Moreover, we will always consider constant  $\bar{g}_x$ s, even though it is more correct in some cases to model  $\bar{g}_x$  as voltage-dependent (e.g., Renart et al (2003)).

#### 3.5.1 Conductance-based LIF neuron

The subthreshold membrane potential of the conductance-based LIF neuron driven by stochastic spike trains as in Sec. 3.3 obeys

$$dV = -\tau^{-1}(V - V_{rest})dt + g_e(V_e - V)dP_e + g_i(V_i - V)dP_i,$$

where  $g_{e,i} = C^{-1}\tau\bar{g}_{e,i}$  are dimensionless peak conductances,  $V_{e,i}$  are the excitatory and inhibitory reversal potentials, and  $dP_{e,i} = \sum_j \delta(t - t_j^{e,i})dt$  are Poisson spike trains with parameter (firing rate)  $v_{e,i}$ . In the diffusion approximation (Sec. 3.2 and 3.3), which heuristically corresponds to replacing  $dP_x$  with  $v_x dt + \sqrt{v_x dt}\xi_t$ , the equation can be put in a form very similar to Eq. 4 (e.g., Hanson and Tuckwell (1983); Lánský and Lánská (1987); Burkitt (2001)); see Table 1. A slightly different model, where the conductances are taken to be OU processes like Eq. 1, has been used by Destexhe and collaborators to recreate the *in vivo*-like activity in neocortical neurons and investigate the role of noisy, background synaptic input on their integrative properties (“point-conductance” neuron, see e.g. Destexhe et al (2001)).

The subthreshold behavior and the response function of the conductance-based neuron (under the approximation discussed in the next subsection) are summarized in Table 1, together with the analogous quantities for the current-based neuron. From the table, it is apparent that the main differences with respect to the current-based IF neuron are: 1) the fluctuations depend on the membrane voltage; 2) an input-dependent, effective time constant  $\tau^*$  appears; 3) the parameter  $\mu$  is *not* the average of the total input current (for example, part of the input contributes to the leak term  $-V/\tau^*$  and is not considered in  $\mu$ ); 4) the voltage is bounded from below by the inhibitory reversal potential (below  $V_i$  inhibitory inputs become excitatory). Usually the last point is taken care of by imposing a reflecting barrier at  $V_i$ , i.e., a hard lower bound for the membrane potential (Hanson and Tuckwell 1983; Lánský and Lánská 1987).

#### 3.5.2 Gaussian approximation for the conductance-based LIF neuron

The analytical form of the response function of this model neuron in the diffusion approximation is known and can be found in e.g. Johannesma (1968) and Richardson (2004). When the diffusion approximation holds, another approximation, called the Gaussian, or ‘effective-time-constant’, approximation, is also valid, and allows for the response function to be put in a form very similar to Eq. 7 (Burkitt et al

**Table 1** Model equations and response function of the current-based and conductance-based LIF neuron (the latter, under the Gaussian approximation; see the text). Subscripts  $e$  and  $i$  stand for “excitatory” and “inhibitory”, respectively. Parameters defining the model neuron:  $V_{rest}$ , resting membrane potential,  $\tau$ , membrane time constant,  $C$ , membrane capacitance,  $\theta$ , threshold for spike emission,  $V_r$ , reset voltage after spike emission,  $\tau_r$ , absolute refractory period,  $V_{e,i}$ , reversal potentials. Parameters defining the input:  $\hat{J}_{e,i}$ , synaptic weights in units of voltage,  $g_{e,i} = C^{-1} \tau \bar{g}_{e,i} > 0$ , dimensionless peak conductances ( $\bar{g}_{e,i}$ , peak conductances),  $v_{e,i}$ , firing rate of afferent neurons. The input parameters in units of current are given, in both cases, by  $m_I = C\mu$  and  $s_I = C\sigma/\sqrt{2\tau^*}$ , with  $\tau^* = 1$  ms. Note that  $\sigma$  depends on  $V$  in the conductance-based model.

symbol	description	current-based	conductance-based	units
	subthreshold Eq. for $V$	$dV = -\frac{V}{\tau} dt + \mu dt + \sigma \sqrt{dt} \xi_t$	(same)	voltage
	conditions for a spike	if $V(t') = \theta \rightarrow$ spike, $V = V_r$ for $t \in ]t', t' + \tau_r[$	(same)	
$\mu$	infinitesimal input current	$\hat{J}_e v_e -  \hat{J}_i  v_i$	$\tau^{-1} V_{rest} + g_e V_e v_e + g_i V_i v_i$	voltage $\cdot$ time $^{-1}$
$\sigma^2$	infinitesimal input variance	$\hat{J}_e^2 v_e + \hat{J}_i^2 v_i$	$g_e^2 (V_e - V)^2 v_e + g_i^2 (V_i - V)^2 v_i$	voltage $^2 \cdot$ time $^{-1}$
$\tau^*$	effective time constant	$\tau$	$(\tau^{-1} + g_e v_e + g_i v_i)^{-1}$	time
$\Phi$	response function	$\left[ \tau_r + \tau^* \int_{V_r}^{\hat{\theta}} \sqrt{\pi} e^{u^2} (1 + \operatorname{erf}(u)) du \right]^{-1}$	(same)	spikes $\cdot$ time $^{-1}$
$\hat{z}$	integrand of response function	$\frac{z - \mu \tau^*}{\sigma \sqrt{\tau^*}}$	$\frac{z - \mu \tau^*}{\sigma(V) _{V=\mu \tau^*} \sqrt{\tau^*}}$	

2003). This form is given in Table 1. The table has been constructed so as to appreciate the formal similarity between the response functions of the current- and conductance-based LIF neurons under this approximation. The Gaussian approximation holds for

$$(g_e^2 v_e + g_i^2 v_i) \tau^* / 2 \ll 1, \quad (9)$$

which is also the limit in which the underlying diffusion approximation holds (Richardson 2004). The condition Eq. 9 is fulfilled under typical cortical conditions (Richardson 2004; La Camera et al 2004a). Heuristically, this approximation amounts to neglecting the dependence of the diffusion coefficient on  $V$ , by replacing  $\sigma(V)$  in Table 1 with its average over the free (i.e., spike-less) process, turning the multiplicative synaptic noise into an additive noise as in the current-driven neuron, see Burkitt et al (2003); Richardson (2004); La Camera et al (2004a); Richardson and Gerstner (2005) for technical details.

### 3.5.3 Equivalence between the response function of the conductance-based and current-based LIF neurons

Networks of current- and conductance-based neurons differ qualitatively in several respects (La Camera et al 2004b; Richardson 2004; Vogels and Abbott 2005; Kumar et al 2008b). However, Table 1 suggests the possibility to “map” one network onto the other so as to have the same input-output relationship in both. Indeed, networks of current- and conductance-based neurons can be made equivalent in terms of the patterns of asynchronous firing rate activity they can express (La Camera et al 2004b). In both the conductance- and current-based IF neuron, the input spike trains were Poisson spike trains characterized by the parameters set  $\Omega \equiv \{v_e, \bar{g}_e, v_i, \bar{g}_i\}$ , which can be taken to define the input. Given the same input  $\Omega$ , it is possible to find a Gauss-distributed current so that

the response function of the current-based neuron,  $\Omega \rightarrow \Phi(\Omega)$ , is the same as the response function of the conductance-based neuron,  $\Omega \rightarrow \Phi_{CB}(\Omega)$ . This holds for both delta-correlated (Rauch et al 2003) and filtered synaptic inputs ( $\tau_I$  of few ms, La Camera et al (2004b)), and requires only a re-definition of the connectivity of the network of current-based neurons.

### 3.6 Firing rate adaptation

When cortical neurons are stimulated with somatic injections of sufficient strength, the initial rate at which action potentials are emitted undergoes a decay with time, a phenomenon called firing rate adaptation (McCormick et al 1985; Lowen and Teich 1992; Fleidervish et al 1996; Sanchez-Vives et al 2000; Reutimann et al 2004; Ulanovsky et al 2004; Descalzo et al 2005; La Camera et al 2006). This decay can occur at different time-scales, and can lead either to a stationary firing rate, as illustrated in Fig. 5, or, if stimulation is sufficiently strong and prolonged, to the complete cessation of spiking activity (Rauch et al 2003).

Firing rate adaptation is ubiquitous in cortical neurons and affects their response to both constant and fluctuating current injections. In models characterized by a threshold-linear response function around the rheobase, firing rate adaptation provides a mechanism for decreasing the slope (or gain) of the response without affecting its sensitivity to input fluctuations (La Camera et al 2002), a property that is necessary for IF neurons to reproduce the response function of cortical neurons (Rauch et al 2003). In models characterized by a highly non-linear response at the rheobase, like the LIF model neuron in the absence of noise (Eq. 8), adaptation removes the singularity and transforms the response function in threshold-linear (Ermentrout 1998). Firing rate adaptation

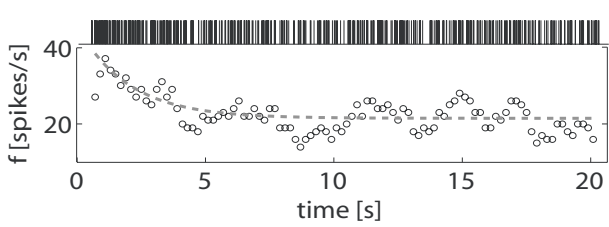


**Fig. 5 Example of firing rate adaption.** A spike train (shown at the top) obtained from a dissociated cortical neuron, cultured *in vitro*, in response to an input current modelled after Eq. 1, see Giugliano et al (2004) for details. In the bottom panel are shown the temporal decay of the instantaneous firing rate, measured as the running average firing rate in a sliding window (circles), and its best exponential fit (dashed line). The output firing rate, initially  $\sim 40$  spikes/s, converges to  $\sim 22$  spikes/s after an exponential decay with time constant of about 2 s. Used and modified with permission from Giugliano et al (2004). Copyright © 2004 by the American Physiological Society.

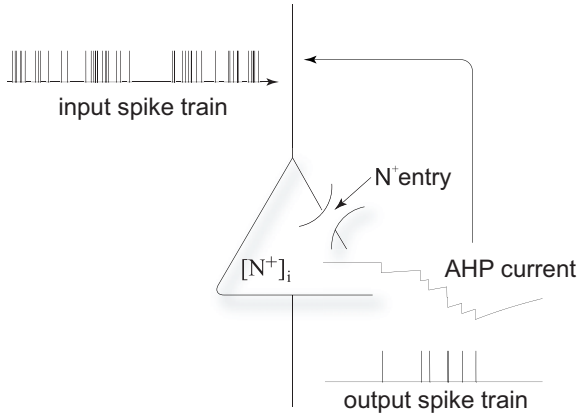


**Fig. 6 Model of firing rate adaptation.** Upon emission of a spike, a quantity of a given ion species  $N$  enters the cell body (triangle) and modifies the intracellular ion concentration  $[N]_i$ , which then exponentially decays to its resting value in a characteristic time  $\tau_N$ , see Eq. 10. Under the conditions discussed in the text, this causes a feedback current proportional to  $[N]_i$  (AHP current), which in turn is responsible for decreasing the output firing rate of the neuron.

also plays a variety of roles in the response to time-varying input current (reviewed in Giugliano et al (2008)). The theory developed so far is extended in this section to include the effect of firing rate adaptation.

### 3.6.1 Minimal model of firing rate adaptation

Firing rate adaptation is a complex phenomenon affected by different ion currents (see Table 1 of Sawczuk et al (1997) for references and a list of possible mechanisms). We describe here a simple model based on a synthesis of the cellular mechanisms underlying adaptation *in vitro*. The model leads to an adapted response function good enough to capture the experimental ones (Rauch et al 2003; La Camera et al 2004a; Giugliano et al 2004; La Camera et al 2006; Arsiere et al 2007). Upon emission of a spike, a quantity  $A_N$  of

a given ion species  $N$  (one can think of  $Ca^{2+}$  or  $Na^+$ ) enters the cell and modifies the intracellular ion concentration  $[N]_i$ , which then exponentially decays to its resting value in a characteristic time  $\tau_N$  (see Fig. 6 for a schematic illustration of this mechanism).  $[N]_i$  dynamics are described by

$$\frac{d[N]_i}{dt} = -\frac{[N]_i}{\tau_N} + A_N \sum_k \delta(t - t_k), \quad (10)$$

where the sum is taken over all the spikes emitted by the neuron up to time  $t$ . As a consequence, an outward,  $N$ -dependent current  $I_{ahp} = -g_N[N]_i$ , proportional to  $[N]_i$  through the average peak conductance  $g_N$ , results and causes a decrease in the discharge rate. This current is commonly given the name of afterhyperpolarization (AHP) (Sah 1996). This term enters the right hand side of Eq. 4 for the membrane potential as

$$dV = -\frac{V - V_{rest}}{\tau} dt - g_N[N]_i dt + \mu dt + \sigma \xi_r \sqrt{dt} \quad (11)$$

with boundary conditions on  $V$  as specified in the absence of adaptation (Sect. 3.3).

### 3.6.2 Mean field theory of firing rate adaptation

For slow enough  $[N]_i$  dynamics, the steady state (ss) intracellular concentration of  $[N]_i$  is proportional to the neuron's output firing rate in a time window of a few  $\tau_N$ :

$$[N]_{i,ss} = \tau_N A_N \sum_{t_k < T} \delta(t - t_k) \approx \tau_N A_N f. \quad (12)$$

This causes a feedback current  $I_{ahp,ss}$  proportional to  $[N]_{i,ss}$ ,  $I_{ahp,ss} = -g_N[N]_{i,ss}$ , which is in general a fluctuating variable because the output spike train is (Fig. 6). Since  $[N]_i$  dynamics are slow,  $I_{ahp,ss}$  is only weakly fluctuating compared to the input current, so that only the mean input current  $m_I = C\mu$  is affected significantly. The total current felt by the neuron, spiking at rate  $f$ , is then  $m_I - \alpha f$ , with  $\alpha = g_N \tau_N A_N$ , plus the fluctuating component which is unaffected by adaptation (the case where this can not be assumed has been studied by Muller et al (2007)). This would cause the neuron to fire at a reduced firing rate  $f_1$ , which in turn causes the mean current to be affected as  $m_I - \alpha f_1$ , and so on. At equilibrium, the adapted firing rate can be numerically obtained by solving the self consistent equation

$$f = \Phi(m_I - \alpha f, s_I), \quad \alpha = g_N \tau_N A_N, \quad (13)$$

which requires only the knowledge of the response function  $\Phi$  and the value of  $\alpha$ . The adapted firing rate is always a stable fixed point of Eq. 13 (La Camera et al 2004a). The adapted response function of the LIF neuron is shown in Fig. 7 (dark curves). It can be noted that firing rate adaptation linearizes Eq. 8 around rheobase (Wang 1998). This result holds for all model neurons whose response function is highly non-linear at rheobase (Ermentrout 1998).

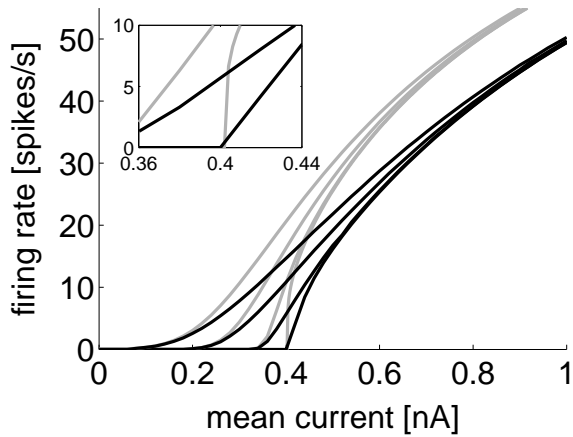


**Fig. 7 Stationary response function of the adapted LIF neuron.** Adapted response function of the white-noise driven LIF neuron, Eq. 13 with  $\Phi$  given by Eq. 7, plotted as in Fig. 4 (dark curves). Same parameters as in Fig. 4, including  $s_I = 0, 0.1, 0.3$  and  $0.5$  nA; adaptation parameter  $\alpha = 4$  pA·s. The non-adapted response function, Eq. 7, is also plotted for comparison (light curves). The rightmost curves are the adapted (dark) and non-adapted (light) response function in the absence of input fluctuations ( $s_I = 0$ ), i.e., Eq. 13 with  $\Phi$  given by Eq. 8 (dark), and Eq. 8 (light), respectively. Adaptation removes the singularity of Eq. 8 by linearizing  $\Phi$  around the rheobase, see the text for details. The *inset* shows an enlargement of the region around rheobase for the curves with  $s_I = 0$  and  $0.1$  nA.

### 3.6.3 Mean field theory of adaptation in the absence of noise

In the absence of noise,  $[N]_i$  dynamics are slow for large  $\tau_N$ , i.e., for  $ISI \ll \tau_N$ , since the ISI sets the time-scale of the output spike train (Ermentrout 1998). For  $\tau_N \sim 100$  ms, the value typically used in modeling studies (Wang 1998; Ermentrout 1998; Liu and Wang 2001), this means that the mean field approximation of the adapted firing rate breaks down below  $1/\tau_N \lesssim 10$  spikes/s. Experimentally, the time constant  $\tau_N$  of the dynamics underlying AHP summation (Eq. 10) is found to vary in a wide range, from tens of milliseconds (fast adaptation) to seconds (slow adaptation), see e.g. Powers et al (1999); La Camera et al (2006). Slow adaptation is naturally amenable to mean field analysis, since a  $\tau_N$  of the order of seconds means a break-down point close to vanishing firing rate. Not so for fast adaptation, however. For e.g.  $\tau_N \sim 20$  ms, in the absence of fluctuations the mean field solution is predicted to break down below 50 spikes/s, which is confirmed by simulations (Fig. 8, compare rightmost curve to symbols). In this case, the adaptation current recovers too quickly to affect the output spike train, contrary to the mean field prediction given by the self-consistent solution of Eq. 13.

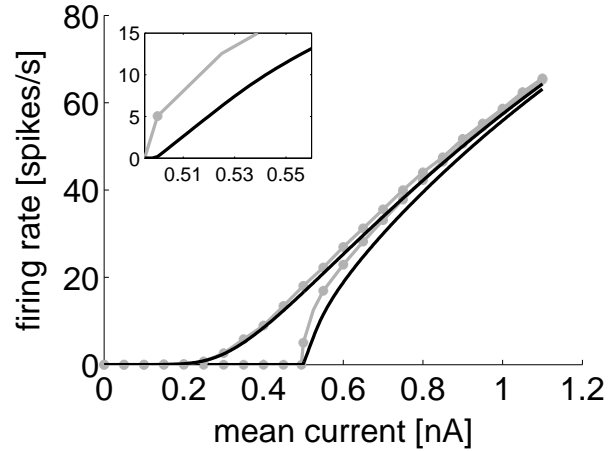


**Fig. 8 Comparison of the mean field theory of firing rate adaptation with simulations.** Response function of the adapting LIF neuron, mean field theory (Eq. 13, dark lines) vs. simulations (Eqs. 10 and 11, light symbols) with  $\tau_N = 20$  ms. The response functions are plotted as in Fig. 4 with  $s_I = 0$  and  $0.4$  nA (from right to left). Neuron parameters were  $\tau = 20$  ms,  $\tau_r = 5$  ms,  $C = 0.5$  nF,  $\theta = 20$  mV,  $V_r = 10$  mV,  $V_{rest} = 0$  mV and  $\alpha = 4$  pA·s. The *inset* shows an enlargement of the region around the rheobase for the curves with  $s_I = 0$ . The mean field approximation in the absence of noise breaks down for  $f \lesssim 50$  spikes/s.

### 3.6.4 Mean field theory of adaptation in the presence of noise

For fast adaptation, the mean field approach should fail also in the presence of fluctuations, since in this case the condition  $ISI \ll \tau_N$  would be replaced by  $\langle ISI \rangle \ll \tau_N$ , where  $\langle \cdot \rangle$  is the average over the spike train. However, it turns out that in a very irregular spike train, Eq. 13 predicts well the adapted firing rate also if condition  $\langle ISI \rangle \ll \tau_N$  is violated (La Camera et al 2004a). This is illustrated in Fig. 8 for  $\tau_N = 20$  (leftmost curve and symbols). In general, the agreement with simulations improves with the amount of input fluctuations, with the break-down point decreasing and approaching vanishing firing rates for large enough fluctuations. This may be due to the fact that, in irregular spike trains, the distribution of ISIs is typically skewed towards values that are smaller than its mean, fulfilling the condition  $ISI \ll \tau_N$  most of the time. A deeper analysis of this phenomenon (and of mean-adaptation theories in general) can be found in Muller et al (2007), and a population density analysis of networks of adapting spiking neurons has been performed by Gigante et al (2007a,b).

### 3.6.5 Adaptive conductance-based IF neuron

The model of firing rate adaptation of Sec. 3.6.2 is easily extended to the conductance-based IF neuron. The adapted response function is given by the solution of the self-consistent equation  $f = \Phi_{CB}(m_I - \alpha f, s_I)$  (La Camera et al 2004a), where  $\Phi_{CB}$  is the response function of the conductance-based

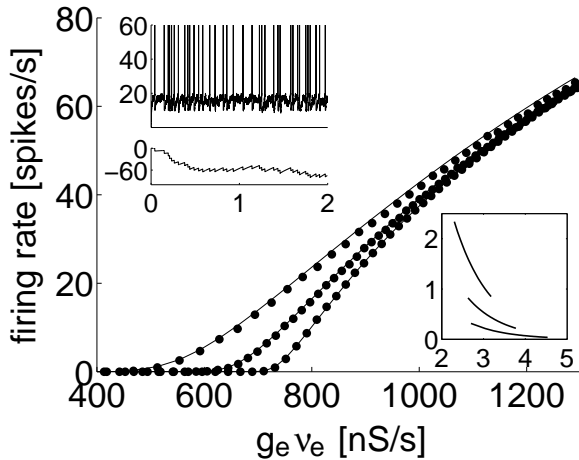


**Fig. 9 Adapted response function of the conductance-based LIF neuron.** Self-consistent solution of  $f = \Phi_{CB}(m_I - \alpha f, s_I)$  (lines) against the simulations (symbols) of the full model (Table 1).  $\Phi_{CB}$  is the response function of the conductance-based LIF neuron in the Gaussian approximation (reported in Table 1). The response functions are plotted as  $\bar{g}_e v_e \rightarrow f$  at constant inhibition, with  $v_i = 500$  spikes/s,  $\bar{g}_i = 1$  nS throughout. Each curve is obtained moving along  $v_e$  and scaling  $\bar{g}_e$  so that  $\sigma_e^2 \equiv \bar{g}_e^2 v_e$  constant ( $\sigma_e = 7.0, 16.9, 33.1$  nS/ $\sqrt{s}$  from right to left), to allow comparison with the current-based neuron in Figs. 4-7 (see Table 1 for an explanation of these symbols). *Right inset:*  $\bar{g}_e$  [nS] as a function of  $v_e$  [spikes/s] plotted as  $\bar{g}_e$  vs  $\log_{10}(v_e)$ . *Left inset:* sample of membrane voltage (mV, top trace) and feedback current  $I_{ahp}$  (pA, bottom trace; see Sec. 3.6.1) as a function of time [s] for the input point with  $\mu_e = 783$  nS/s,  $\sigma_e = 33.1$  nS/ $\sqrt{s}$ . Adaptation parameters:  $\tau_N = 500$  ms,  $g_{NA_N} = 8$  pA (so that  $\alpha = 4$  pA·s). Neuron parameters:  $\tau_r = 5$  ms,  $C = 0.5$  nF,  $\theta = 20$  mV,  $V_r = 10$  mV,  $V_{rest} = 0$ ,  $\tau = 20$  ms,  $V_e = 70$  mV,  $V_i = -10$  mV. Used and modified with permission from La Camera et al (2004a). Copyright © 2004 by The MIT Press.

neuron, and  $m_I$  and  $s_I$  are  $\mu$  and  $\sigma$  from Table 1 in units of current. The agreement with simulations is shown in Fig. 9. To allow for a comparison with the response function of the current-based LIF neuron as shown in Fig. 7, where  $s_I$  is constant in each curve,  $v_e$  was increased while scaling  $\bar{g}_e$  as  $\sim 1/\sqrt{v_e}$ , with  $\bar{g}_i, v_i$  held constant. This corresponds to increasing  $m_I$  (as  $\sim \sqrt{v_e - \bar{g}_i v_i}$ ) at constant  $s_I^2$  ( $\propto \bar{g}_e^2 v_e + \bar{g}_i^2 v_i$ ) in the current-based neuron (see Table 1).

### 3.6.6 Other models of adaptation

Other models of firing rate adaptation are also in use in the literature, among which an adapting threshold for spike emission (e.g., Holden (1976); Wilbur and Rinzel (1983); Liu and Wang (2001); La Camera et al (2004a)) which is amenable to the mean field approach described in this section. The LIF neuron, endowed with such a mechanism, was found equally able to fit the response function of rat pyramidal neurons as did the model with AHP adaptation (La Camera et al 2004a). AHP Adaptation, however, is a more general mechanism and, in some sense, universal, in that most adapting currents can be described by such a mechanism under reasonable assumptions (Benda and Herz 2003). Other types

of adaptation phenomena, for example due to slow inactivation of  $Na^+$  channels (Fleiderovich et al 1996), are present in cortical neurons, and some can also be treated within the mean field approach as done for AHP-dependent adaptation, sometimes leading to qualitatively new phenomena like non-monotonic response functions (Giugliano et al 2002).

## 4 Applications of the theory of cortical response function

Many properties of the behavior of networks of spiking neurons can be predicted from the knowledge of the single-neuron response function. In this section we will review briefly some of those properties related to the attractive dynamics of recurrent networks, such as the possibility of the coexistence of spontaneous and stimulus-selective persistent activity in the interval between two relevant events (Amit and Brunel 1997b; Brunel 2000a), the characteristic times governing the transient response of the network to a stimulus (Mattia and Del Giudice 2002; Renart et al 2003), and the dynamics leading to perceptual, motor, or rule-based decisions (Rolls and Deco 2001).

### 4.1 Attractors of the neural dynamics

Under the mean field assumption of Sec. 3.1, the shape of the response function can be used to predict the stable ‘fixed points’ of the dynamics of neural populations, also called ‘attractors’ because the collective activity of the population, if close to the activity defined by those fixed points, tends to merge into it. These attractors can be visualized as the intersections of the response function with the unit straight line, as shown in Fig. 10A. In the figure, both the input (horizontal axis) and the output (vertical axis) is the firing rate of the entire population, which in the logical construction of mean field theory coincides with the firing rate of any representative neuron (see Sec. 3.1). At the points in which the response function (thick or thin curve) intersects the dashed straight line, the output rate of each neuron of the population equals its input rate. These fixed points are the attractors of the population dynamics. Fixed points at which the slope of the response function is smaller than 1 are stable attractors, meaning that the collective behavior of the network in this state is resumed after a temporary disturbance due to small perturbations.

Since the parameters of the neuron and the properties of the synaptic connections shape the response function (two examples, the thick and the thin curves, are shown in Fig. 10A), the response function can be used to infer the dynamical properties of neural populations and, thus, of cortical circuits. We illustrate how with a few examples in the next subsections, where we use the response function to infer the possibility that the network can sustain a state of so-called ‘persistent activity’ in one or more firing rate regimes.

## 4.2 Spontaneous activity

A spontaneous, not stimulus-driven neural activity at low firing rates has been interpreted as a global attractor of a recurrent network of spiking neurons (Amit and Brunel 1997b). This activity is the result of the interaction between excitatory neurons, it is self-sustaining both in the presence and in the absence of an external synaptic input, and is highly irregular due to the disorder of synaptic connections (van Vreeswijk and Sompolinsky 1996). The type of synaptic drive, current-based vs. conductance-based, can play a decisive role (Vogels and Abbott 2005; Kumar et al 2008b). For conductance-based inputs, spontaneous activity can persist for long periods of time even in the absence of external inputs. The survival time of self-sustained activity increases exponentially with network size (Kumar et al 2008b).

We base the examples of this section on networks of current-driven LIF neurons. In the absence of noise, or when the model neurons are insensitive to input fluctuations, the activity either dies out or converges onto a pattern of firing rates that are significantly higher than those typically observed in cortical recordings in behaving animals (Miyashita and Chang 1988; Amit and Brunel 1997b; Yakovlev et al 1998). Both possibilities can be predicted by the shape of the response function as illustrated in Fig. 10A (thin curve). For a collective activity above that represented by the open circle, the activity will converge towards a higher activity state (“\*”). Similarly, an initial activity below the same critical point will eventually die out, i.e., all neurons will stop firing (the zero output rate in figure). This is because the open circle represents a unstable fixed point of the population dynamics.

In the presence of fluctuations, however, it is possible to have a state of spontaneous activity at low firing rates, like the closed circle marked “SA” in Fig. 10A. Notice the two main ingredients for a finite spontaneous activity to be stable in a single excitatory network of current-driven LIF neurons: a change in convexity around rheobase due to the sensitivity to input fluctuations (see the inset of Fig. 10A), and the presence of an external input (so that for a null recurrent input the output firing rate of the population is higher than zero, as shown in figure). If any of these ingredients is lacking, the quiescent state is the only stable fixed point at low firing rates in such a network.

## 4.3 Stimulus-selective persistent activity

The two closed circles that mark the intersection of the thick response function with the straight line in Fig. 10A are both stable attractors, or stable states of persistent activity. In principle, any self-sustained network activity is to be labelled as persistent activity, and that includes spontaneous activity, persistent activity at higher firing rates, and the inter-trial activity found in infero-temporal cortex of behaving macaques (Yakovlev et al 1998). However, it is common in the literature to refer to persistent activity as to self-sustained activity

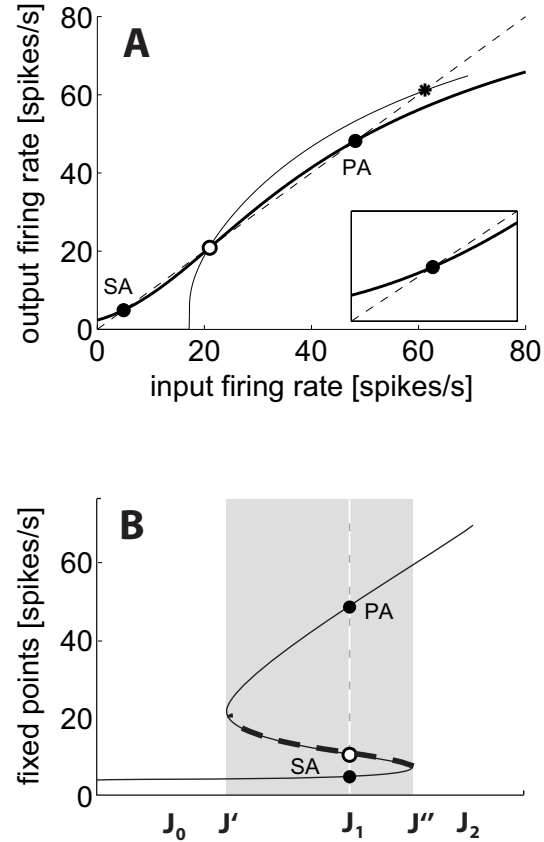


**Fig. 10 Prediction of network behavior by means of its single neurons’ response function.** **A.** At the points in which the response function (thick or thin curve) intersects the straight line (dashed), the output rate of each neuron of the population equals its input rate (fixed points of the population dynamics). In the case of the LIF neuron driven by a noiseless input current (thin curve, Eq. 8), the activity either dies out to zero firing rate or converges onto a pattern of firing rates that are significantly higher than those typically observed in cortical recordings *in vivo* (“\*”). In the presence of input fluctuations (thick curve, Eq. 7), two stable points of self-sustained network activity can be found if appropriate synaptic weights are chosen, which we call spontaneous activity (“SA”,  $\sim 5$  spikes/s), and persistent activity (“PA”,  $\sim 50$  spikes/s). The open circle is an unstable fixed point. *Inset:* enlargement of the region around SA showing that the slope of the response function is less than 1 at this point. **B.** Fixed points of the network in A (thick curve) as a function of the average recurrent synaptic weights  $J$ . Coexistence of spontaneous and persistent activity is possible in the interval  $[J', J'']$  (shaded area). The dark dashed curve is the ‘unstable manifold’, i.e., the continuous collection of all unstable fixed points in the bistable region. The three fixed points shown in A are obtained for  $J = J_1$ . For  $J < J'$  (for example, at  $J_0$ ), only spontaneous activity is stable, whereas for  $J > J''$  (for example, at  $J_2$ ), spontaneous activity is destabilized and only persistent activity at high firing rate is stable.

that i) is expressed at higher firing rates than spontaneous activity and ii) that can be obtained in a neural subpopulation on top of, and without disrupting, the spontaneous activity of the embedding network (Amit and Brunel 1997b). Sometimes, the property of being stimulus-selective is also assumed, that is, the state of persistent activity must be ignited by the transient presentation (or the activation of an

internal representation) of a particular class of stimuli, and not just any stimulus. According to this definition, the low rate stable point marked “SA” in Fig. 10A can be interpreted as the state of spontaneous activity, whereas the high rate point (PA) can be interpreted as a state of persistent activity. Indeed, the activity in state PA occurs at higher firing rate than SA, and its presence does not destabilize SA (and viceversa).

The conditions for stable coexistence of spontaneous and persistent activity can be stated in terms of the parameters defining the network (in particular, the synaptic strength), and can be predicted from the way a parameter change shapes the single neurons’ response function. In general, it is desirable that the coexistence of both fixed points can be found in a whole interval of potentiated synaptic values. The procedure for finding such interval involves the response function and is best visualized with the help of bifurcation diagrams (e.g., Amit and Brunel (1997b); Brunel (2000b); Del Giudice et al (2003)). These diagrams depict the fixed points of the network as a function of the strength of the synaptic couplings, as illustrated in Fig. 10B. When the synaptic couplings are not potentiated enough, only the spontaneous activity state can be stable (the region to the left of  $J'$ ). When synaptic strength is potentiated, thought of as the signature of some learning process, a second stable fixed point can be found at higher firing rate, for example the point marked ‘PA’. For yet stronger synapses (the region to the right of  $J''$ ), the spontaneous activity state loses its stability and only the higher rate persistent activity is stable. Bistability can occur for any value of the potentiated synaptic strength in the interval  $[J', J'']$ : the larger this interval, the more robust the phenomenon.

Stimulus-selective persistent activity has been put forward as a potential neural correlate of working memory of sensory stimuli in prefrontal, infero-temporal and posterior parietal cortex (Amit and Brunel 1997b). More specifically, it is a model for delay activity, the neural activity observed between two relevant events in the absence of external stimulation (e.g., Fuster and Jervey (1981); Miyashita (1988); Miyashita and Chang (1988); Funahashi et al (1989); Koch and Fuster (1989); Wilson et al (1993); Yakovlev et al (1998); for a review see Fuster (1995)). There is some experimental support to the idea that the stimulus-selective activity observed in infero-temporal cortex in 2-8 seconds delays during a delayed-matching-to-sample task is the result of the collective attractor behavior of large populations of neurons (Amit et al 1997; Yakovlev et al 1998). The use of the response function to locate these attractors can be applied to networks with an arbitrary number of sub-populations (Amit and Brunel 1997b; Mascaro and Amit 1999; Brunel 2000a), also when the sub-populations share neurons coding for the same subgroup of stimuli (La Camera 1999; Curti et al 2004), and can be generalized to include firing rate adaptation with the procedure of Sec. 3.6.2.

#### 4.4 Network response to time varying inputs

So far (and in the remainder of this manuscript) we have been concerned with stationary properties of the response of cortical neurons (Sec. 3). The network dynamics can be studied in the framework of mean field theory also when the input statistics are not stationary. Some of these extensions are reviewed in Giugliano et al (2008); here we mention briefly a few applications of the stationary response function to the characterization of the transient behavior of the network and its response to time-varying inputs.

For delta-correlated synaptic currents, the network response to time varying inputs can be studied analytically under specific simplifying assumptions and it is in general rather complicated. The response time of the network in general depends on the full distribution of the depolarizations ( $V - V_{rest}$ ) of all the neurons. For example, networks with spontaneous activity react much faster than networks that are completely silent, as many neurons are close to the threshold for emitting a spike and they can contribute to increasing rapidly the population firing rate (Amit and Brunel 1997a,b; Fusi and Mattia 1999; van Rossum et al 2002). When the distribution of depolarizations is important, the mean field approach requires the solution of a full Fokker-Planck equation describing the time development of the population density (Knight 1972a; Fusi and Mattia 1999; Brunel and Hakim 1999; Nykamp and Tranchina 2000; Mattia and Del Giudice 2002). In some cases, however, the transient dynamics can be simplified to the point that it mostly depends on the slope of the stationary response function  $\Phi(m_I, s_I)$  (Mattia and Del Giudice 2002).

For more realistic synaptic currents, the study of transients can be further simplified. If the network dynamics are faster than the integration time constants of the synaptic currents, it is often safe to assume that the network is constantly at the equilibrium point of the Fokker-Planck equation (Renart et al 2003; La Camera et al 2004a). This means that for every synaptic input, we can replace the instantaneous firing rate with the firing rate given by the stationary response function. For realistic conditions, the reaction time of networks of IF neurons (a few milliseconds) is shorter or comparable to the integration time constants of AMPA- and GABA<sub>A</sub>-, and much shorter than the dynamics of NMDA- and GABA<sub>B</sub>-receptor-mediated current (from tens to hundreds of milliseconds). This approximation is usually good for signals that vary on time-scales of tens of milliseconds and this approach is similar to the one described for adaptation in Sec. 3.6. A similar approximation can be used in the presence of short-term (Tsodyks and Markram 1997; Tsodyks et al 1998; Mongillo et al 2008) or long term synaptic plasticity (Del Giudice et al 2003; Amit and Mongillo 2003). For faster inputs a different approach is required and is reviewed in Giugliano et al (2008).

These and other examples show that the stationary response function, which by definition is supposed to characterize only stationary network states, can also be used to infer some of the dynamic behaviors of networks.

#### 4.5 Decision making in cortical circuits

In the case of ambiguous or barely perceivable sensory stimuli, we are sometimes required to make a decision about the identity of the stimulus and generate a particular percept. Such a process is similar to the selection of an action in response to the occurrence of one or more events and it is also part of the cognitive processes related to decision making. In recent models, each possible decision has been associated with a particular attractor of the neural dynamics, representing e.g. perceptual decisions (Wang 2002; Wong and Wang 2006), decisions about actions in response to visual stimuli (Fusi et al 2007), and rule-based decisions such as those occurring in cognitive tasks like the Wisconsin Card Sorting Test (Rolls and Deco 2001). The same approach can be used in general models of working memory in which every mental state is an attractor of the neural dynamics and it represents a particular disposition to behavior (Rigotti et al 2008). Relevant events or sensory stimuli trigger a competition between the neural populations corresponding to different percepts or actions. The competition results from the recurrent self-excitation of each decision population and the mutual suppression due to inhibitory neurons. The stable fixed points of the dynamics correspond to particular decisions that are mutually exclusive. As in the case of stimulus-selective delay activity, the set of equilibrium points corresponding to the attractors can be studied with a mean field approach and are related to the properties of the single-neurons' response functions.

Other potential applications of the concept of response function are related to the role played by gain modulation (Salinas and Thier 2000; Salinas and Sejnowski 2001; Larkum et al 2004), balanced synaptic inputs (Burkitt 2001; Burkitt et al 2003), and neuromodulators (Brunel and Wang 2001; Thurley et al 2008) in the dynamics of cortical circuits.

### 5 The response function of cortical neurons

The applications of the mean field approach and the concept of response function reviewed in the previous section depend on several assumptions; in particular, on the assumption that the neurons can be described as IF neurons, or at least that their response can be accurately predicted by the response function of IF neurons. This warrants investigation of whether or not this fundamental assumption is correct. Is the response of cortical neurons to *in vivo*-like input current well described by the response function of IF neurons? If yes, which type of cortical neurons? Which type of IF neuron? And how accurate the predictions of the theory are? Recently, quantitative answers have been given to all of these questions in rat cortical neurons of the pyramidal and fast-spiking (FS) type in layer 2/3 (L2/3) and layer 5 (L5) of somatosensory cortex (SSC), in rat pyramidal neurons of L2/3 of medial prefrontal cortex (mPFC), and in neurons from dissociated cultures of rat neocortex. In this section, we review briefly the main results, starting from the essen-

tial facts regarding the experimental and fitting procedures. The reader is referred to the original papers for a more comprehensive account (Rauch et al 2003; Giugliano et al 2004; La Camera et al 2006; Arsiero et al 2007).

#### 5.1 Experimental and fitting procedures

An *in vivo*-like current modelled after Eq. 1 was injected into the soma of the neurons in the current clamp configuration, and the membrane potential was recorded from the same electrode. Recordings were performed at  $\sim 35^\circ\text{C}$  in all studies apart from the case of cultured neurons (Giugliano et al 2004), where they were performed at room temperature. The dendrites were cut to ensure that the only source of input fluctuations came from the injected current, so as to allow for complete control of the input and to prevent the generation of non-linear dendritic events like calcium spikes (Larkum et al 1999, 2004). The correlation length of the current,  $\tau_I$  in Eq. 1, was between 1 and 10ms (mostly 1ms). The parameters  $m_I$  and  $s_I$  were chosen randomly for each recording, from a pre-defined pool of values which had been previously shown to drive the target neurons within their physiological range. Given that  $\tau_I$  was constant for each cell, the current was characterized by the pair  $\{m_I, s_I\}$ . The same pair was used from one to five times for each cell, to control for the stability of the recordings (in terms of membrane resistance, spike shape, and firing rate). Each repetition, however, used a new realization of the random noise,  $\xi_t$  in Eq. 1. If the percentage of unstable recording was above a given threshold, the cell was declared unstable and was not considered for further analysis. A second criterion to be passed was the quasi-stationarity of the response. The firing rate of the neuron was considered quasi-stationary if its value in the last second of stimulation was within a given range of the firing rate in the first second of stimulation, despite firing rate adaptation (present also in stable recordings). The duration of each recording was of the order of seconds, from a minimum of 4 to a maximum of 60 seconds, to ensure that the response would settle into its quasi-stationary regime. Most recordings used durations of the order of 10 seconds. In some cases, the duration was adaptively adjusted depending on the firing rate of the neuron. For stable cells, repetitions across  $\{m_I, s_I\}$  pairs (when available) were averaged, and the average was taken as the mean firing rate in response to the injected current. Given the small number of repetitions, and the fact that at small firing rates the Gaussian model of random errors does not hold for probabilities, the confidence interval around the measured firing rate,  $\Delta f$ , was not given by the standard error of the mean. Instead, a binomial model for the emission of a spike in a tiny interval was used to derive an adaptation of the Wilson 'score' equation (Meyer 1965; Brown et al 2001) with a limiting procedure on the duration of the binning interval (La Camera et al 2006). The theoretical adapted stationary response function (Eq. 13 with  $\Phi$  given by Eq. 7) was fitted to the experimental quasi-stationary firing rates, via a least-square minimization

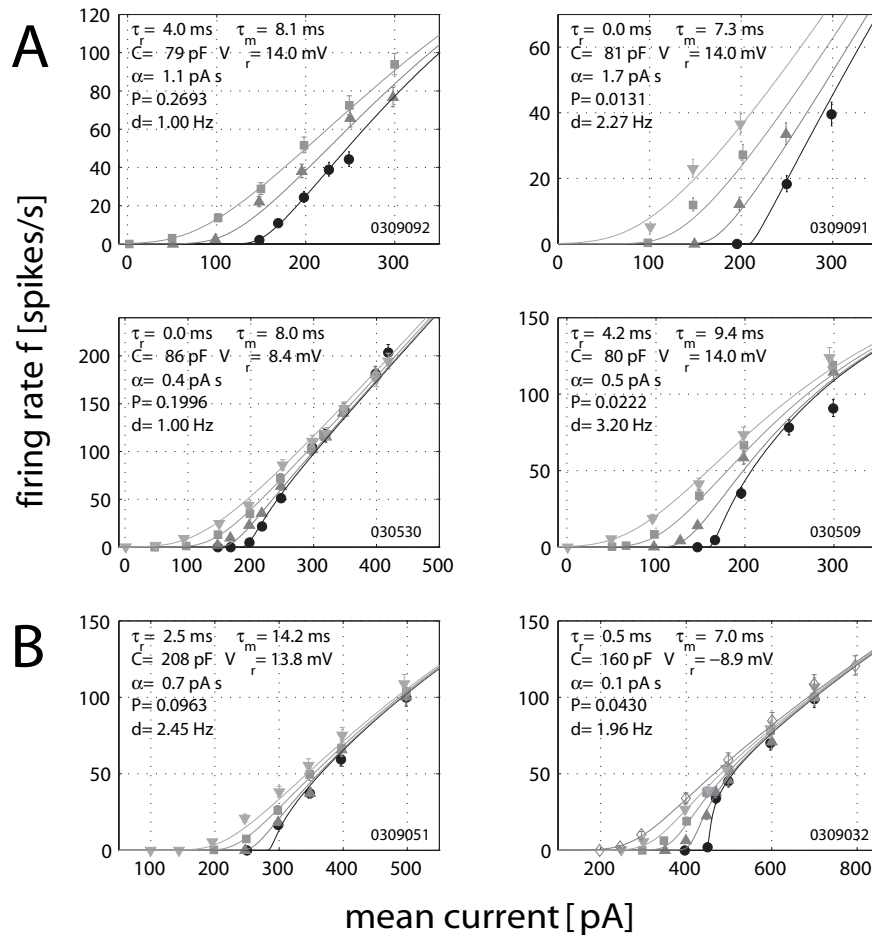


**Fig. 11 Response functions of FS neurons.** Best-fits of the adapted LIF response function, Eq. 13 with  $\Phi$  given by Eq. 7, to the experimental response of four FS interneurons from L5 (**A**) and two interneurons from L2/3 (**B**) of rat SSC. Symbols are experimental quasi-stationary firing rates, full lines are the model fits to the data. The output firing rates are plotted as in Fig. 4, with  $s_I$  that ranged from 10 to 200 pA (see Fig. 3 of La Camera et al (2006) for details). The best fit parameters are reported in the left top corner of each plot (the average best fit parameters across fitted cells are reported in Tab. 2).  $P$  is the probability that a  $\chi^2$  variable with the same number of degrees of freedom is larger than the best-fit one. A fit was accepted if  $P > 0.01$ .  $d$  is the absolute discrepancy, i.e., the average (across all points) absolute difference between the measured and the theoretical frequencies of the best-fit curves. Used and modified with permission from La Camera et al (2006). Copyright © 2006 by the American Physiological Society.

of  $\chi^2 = \sum_i \left( \frac{f_i^{th} - f_i^{exp}}{\Delta f_i} \right)^2$ , where  $f_i^{th}$  and  $f_i^{exp}$  are the theoretical and experimental firing rates, respectively, and the sum runs over all data points. Minimization was achieved by tuning the neuron parameters in Eq. 7 and the adaptation parameter  $\alpha$  of Eq. 13 with a Montecarlo procedure. Since  $\theta$ ,  $V_r$  and  $C$  are not independent parameters (in Eq. 7 they appear always in the form  $C\theta$  and  $CV_r$ ),  $\theta$  was set arbitrarily to 20 mV in all studies. Finally, notice that due to the use of finite (albeit small)  $\tau_I$  for the current Eq. 1, the corrected version of the response function given in Brunel and Sergi (1998); Fourcaud and Brunel (2002) should be used in place of Eq. 7 (see also Sec. 3.4). However, this correction predicts a phenomenon, the crossing of  $f$ - $I$  curves with different  $\sigma$ s for large input current, which was not observed in the exper-

iments (Rauch et al 2003; Giugliano et al 2004; La Camera et al 2006; Arsiero et al 2007). For this reason, and given that  $\tau_I$  was extremely small ( $= 1$  ms) in most cases, Eq. 7 was preferred in fitting the theory to the data.

## 5.2 Fast-spiking neurons

The experimental response functions of rat FS interneurons in L2/3 and L5 of SSC of the rat are shown in Fig. 11 (symbols). The response functions in the two layers were only slightly different. Up to all frequencies which are sustainable by the neuron, the response function was very well described by the adapted response function of the LIF neuron, i.e., Eq. 13 with  $\Phi$  given by Eq. 7 (lines in Fig. 11)

(La Camera et al 2006). A discrepancy was observed between the effective parameters of the neurons (i.e., the best-fit parameter values of the capacitance and membrane time constant) and the same parameter values estimated more directly through a classical impulsive- and step-protocol procedure. This means that, for the IF neuron to reproduce the response of real neurons, *effective* parameters must be used (see Tab. 2). Such parameters compensate for the lack of biophysical detail and other simplifications made in IF neurons (e.g., real neurons are not point neurons nor are electrotonically compact).

### 5.3 Pyramidal neurons

#### 5.3.1 Pyramidal neurons from the somatosensory cortex of rats

The response function of pyramidal neurons from L5 of rat SSC was well described by the response functions of the LIF neuron (see Rauch et al (2003) for examples). A second type of IF neuron, the linear IF neuron with a floor (Abbott and van Vreeswijk 1993; Fusi and Mattia 1999), also gave a good description (Rauch et al 2003). This model neuron, however, described less well the response function of cultured neurons (Giugliano et al 2004), and were not suited to describe the response of FS neurons (La Camera et al 2006). The effective parameters of the LIF neuron were different from, and not correlated with, the directly-estimated parameters of the real neurons in acute slices, but were rather close to the directly estimated parameters in cultured neurons. This could be explained by the compactness and smaller size of the cultured neurons, making the point-approximation implicit in the model work better (this argument, however, does not seem to hold for FS neurons). Pyramidal neurons of the SSC were not very sensitive to the effect of input fluctuations, especially if compared to FS neurons and pyramidal neurons of the mPFC. A more complete comparison is given in a later section.

#### 5.3.2 Pyramidal neurons from the medial prefrontal cortex of rats

Many pyramidal neurons in L5 of the rat mPFC (Fig. 12, symbols) displayed a sensitivity to input fluctuations far greater than predicted by the theory developed in Sec. 3 (cfr. Eq. 7 and Fig. 7) resulting in a saturating and 'divergent' response function (Arsiero et al 2007). These neurons retain a large dependence on input fluctuations well above threshold and, in fact, close to saturation, where an additional increase of the average input will not cause any increase of the output firing rate. The resulting shape of the response function is still convex near threshold, but divergent in the high output rate range (Fig. 12). The phenomenon is possibly due to after-hyperpolarization currents (Higgs et al 2006) as well as to the slow inactivation of sodium channels (Arsiero et al 2007). In support of this hypothesis, the response function

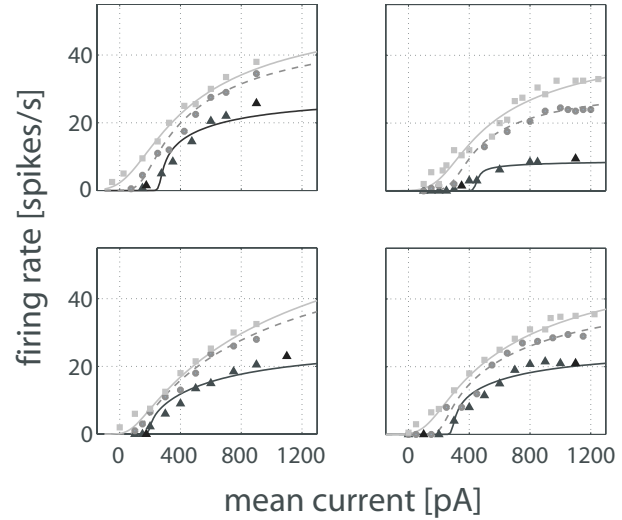


**Fig. 12 Response functions of rat medial prefrontal cortex.** Response function and IF model reduction of four mPFC L5 pyramidal neurons. Fitting procedure and plots as in Fig. 11. The model response function is defined by the self-consistent solution of  $f = \Phi(m_I - \alpha f, s_I, \tau_r(s_I))$ , where  $\Phi$  is the response function of the LIF neuron, Eq. 7, and  $\tau_r(s_I) = \tau_r + \omega/s_I$  is a fluctuation-dependent refractory period. The  $\omega$ -dependent model was used to account for the divergence of the response curves at large input current for different amplitudes of the input fluctuations (from right to left,  $s_I = 50, 150$  and  $300$  pA). Reproduced and modified with permission from Arsiero et al (2007). Copyright © 2007 by the Society for Neuroscience.

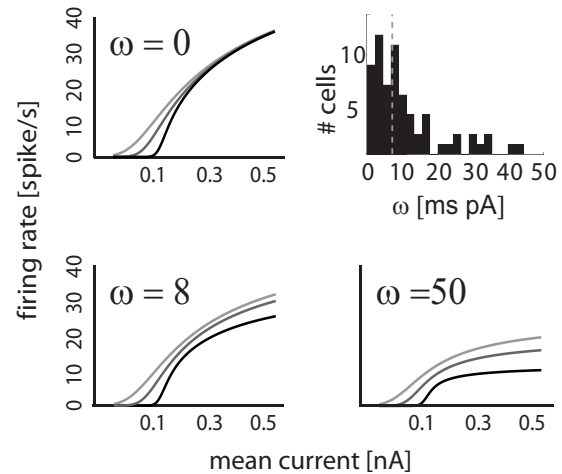


**Fig. 13 Role of parameter  $\omega$  in the high output rate regime of neocortical neurons.** Pictorial response functions plotted as in Fig. 4 for three different values of  $s_I$  (in each plot) and  $\omega$  (in different plots). Top right:  $\omega$ 's best-fit values in pyramidal neurons from L5 of mPFC of the rat (see Fig. 12 for a few examples). The larger  $\omega$ , the more divergent the response curves at large input current for different amplitudes of the input fluctuations. Reproduced and modified with permission from Arsiero et al (2007). Copyright © 2007 by the Society for Neuroscience.

**Table 2** Best-fit parameters of the adaptive LIF neuron to the experimental response functions of neurons from several areas of rat neocortex. Parameters values are reported as mean  $\pm$  SD. Parameters are as defined in Sec. 3.3:  $\tau$ : membrane time constant;  $C$ , membrane capacitance,  $V_r$ : reset voltage after spike emission,  $\tau_r$ : absolute refractory period.  $\alpha$  is the adaptation parameter defined in Eq. 13, and  $\omega$  is the divergence factor defined in Sec. 5.3.2. The threshold for spike emission,  $\theta$ , was set arbitrarily to 20 mV in all cases (see Sec. 5.1 for details). A positive  $\omega$  for the mPFC neurons means that the response at large input current differed for different amounts of input fluctuations, see the text for details. The  $\omega$ -dependent model was not used in the other cases (-).

	FS, L5	FS, L2/3	PYR, L5	PYR, L5 (mPFC)	cultured
$\alpha$ [pA s]	$0.8 \pm 0.5$	$1.0 \pm 0.9$	$10.8 \pm 6.3$	$3.9 \pm 2.5$	$6.4 \pm 4.5$
$\tau_r$ [ms]	$1.4 \pm 2.1$	$3.3 \pm 2.6$	$9.4 \pm 6.5$	$12.5 \pm 4.2$	$23.0 \pm 22.6$
$V_r$ [mV]	$8.8 \pm 9.4$	$5.3 \pm 11.3$	$9.9 \pm 10.2$	$1.3 \pm 4.3$	$10.6 \pm 14.1$
$\tau$ [ms]	$7.5 \pm 1.5$	$8.3 \pm 3.6$	$26.3 \pm 13.2$	$30.1 \pm 11.3$	$30.1 \pm 21.4$
$C$ [pF]	$80 \pm 13$	$140 \pm 48$	$530 \pm 290$	$285.1 \pm 111.2$	$86.5 \pm 56.6$
$\omega$ [ms/pA]	-	-	-	$14.3 \pm 19.7$	-

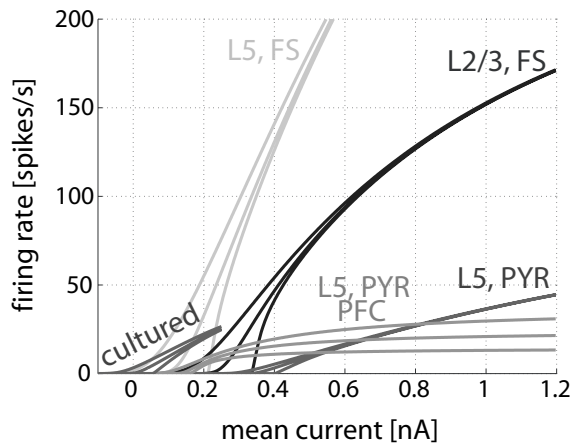


**Fig. 14 Response functions of pyramidal and FS neurons.** Comparison between the quasi-stationary response functions of FS neurons of L5 and L2/3 of SSC (La Camera et al 2006), pyramidal (PYR) neurons from SSC (Rauch et al 2003) and mPFC (Arsiero et al 2007), and dissociated cultures of rat neocortex (Giugliano et al 2004). The steady state responses were obtained using the average best-fit parameters of Table 2 with  $s_I = 0, 0.1, \text{ and } 0.2$  nA, and are plotted as in Fig. 4. Used and modified with permission from (La Camera et al 2006). Copyright © 2006 by the American Physiological Society.

#### 5.4 Comparison among the response functions of pyramidal and FS neurons

Fig. 14 shows the comparison between the response functions of pyramidal and FS neurons. In each class, the response function was obtained by using the average best-fit parameters across cells reported in Table 2, and three values of  $s_I$  were used in each case to show the dependence on the input fluctuations. The ranges of both the average and the variance of the current cover the actual physiological ranges found in the experiments. The maximal output firing rates in figure are the maximal firing rates sustainable by the neurons during the experiments. Thus, Fig. 14 provides at a glance a comparison of the ‘average’ response function of neurons from different preparations, together with their physiological range of operation in response to *in vivo*-like input current.

It can be noted that the maximal firing rate sustainable by FS neurons is much larger than in pyramidal neurons ( $\sim 200$  spikes/s vs.  $\sim 50$  spikes/s). Moreover, FS neurons have a much larger response to fluctuations at rheobase, and a smaller effective  $C$ ,  $\tau$  and  $\tau_r$  (Table 2). Overall, these results imply that FS neurons respond faster and to a much higher extent to input changes than pyramidal neurons.

#### 5.5 Variability of the inter-spike intervals

of a Hodgkin-Huxley model endowed with slow inactivation of sodium channels exhibits the same properties (Arsiero et al 2007). The LIF neuron endowed with a refractory period that readjusts its value depending on the variance of the input is a minimal spiking model able to capture this phenomenon. In such a model, the absolute refractory time results from the sum of two contributions: a constant term,  $\tau_r$ , and a term  $\omega/s_I$ , decreasing with  $s_I$ :  $\tau_r(s_I) = \tau_r + \omega/s_I$ . The effective refractory period is thus smaller for larger fluctuations, increasing the firing rate in response to the same mean input, as shown in Fig. 13. The adapted response function for this model fits well the experimental functions measured in mPFC (Fig. 12) and allows for several predictions to be made about the behavior of networks of mPFC neurons (Arsiero et al 2007).

The coefficient of variability (CV), defined as the ratio between the standard deviation and the average of the ISIs, was used to assess the spike train variability (Stein 1965; Reich et al 1997; Gabbiani and Koch 1998; Shadlen and Newsome 1998; Kostal et al 2007). Strictly speaking, this measure can be meaningfully applied only to stationary or quasi-stationary spike trains (see Sec. 2.2), which is the case we consider in this article. Two typical cases for FS interneurons are shown in Fig. 15 for one L5 (left) and one L2/3 (right) interneuron, together with the prediction of the LIF model neuron whose parameters were tuned to fit the firing rates only (full lines). The variability of FS neurons are contrasted in the same figure with the typical variability of pyramidal neurons from SSC and mPFC (dashed lines). The comparison shown in the figure confirms the larger sensi-

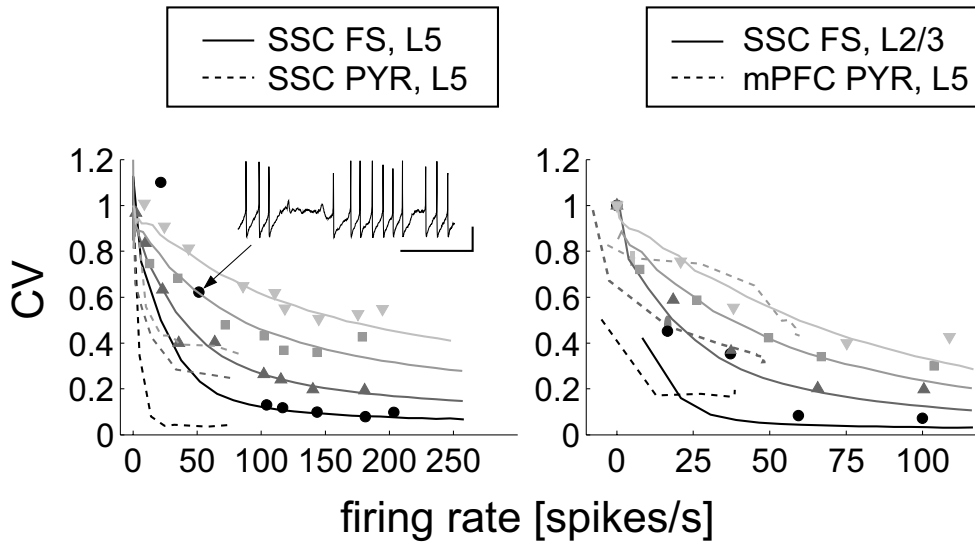


**Fig. 15 Coefficient of variability (CV) of pyramidal and FS neurons.** Comparison of CV of FS (full lines and symbols) and pyramidal (PYR) neurons (dashed lines) from SSC (left) and mPFC (right) of the rat. Symbols (FS) and dashed lines (PYR) are experimental data for a representative neuron in each class; full lines are the best fits of the CV of the LIF model neuron to the data from FS neurons (symbols). CV values are plotted as a function of the neuron's output rate at constant magnitude of the input fluctuations,  $s_I$ , with (from bottom to top):  $s_I(FS, L5) = 20, 50, 100$  and  $150$  pA;  $s_I(FS, L2/3) = 10, 50, 100$  and  $150$  pA;  $s_I(SSC, PYR) = 50, 150$  and  $300$  pA;  $s_I(mPFC, PYR) = 50, 150$  and  $300$  pA. Different fluctuations' ranges were used in different preparations due to different physiological properties of the neurons (note the different scales for the horizontal axis). In the fitting procedure, the neuron parameters were tuned to match both CV and firing rate for all data points, i.e., for all  $\{m_I, s_I\}$  pairs used for each fitted cell. For both fitted FS cells shown here, the adaptive LIF neuron with  $\tau_\alpha = 500$  ms was used. *Inset:* segment of the voltage trace for the point indicated by the arrow (calibration bars: 100 ms and 20 mV). The CV of this point is enhanced by the "stuttering" behavior of the spike train and can not be captured by the model. Used and modified with permission from (La Camera et al 2006). Copyright © 2006 by the American Physiological Society.

tivity to fluctuations in FS neurons, compared to pyramidal neurons, implied by the shape of the response functions shown in Fig. 14. Although the variability of mPFC pyramidal neurons is higher than in SSC, and contrary to the effect on the firing rate (Sec. 5.3.2), the sensitivity of the CV to the input fluctuations is comparable in SSC and mPFC (dashed lines in both panels).

## 6 Discussion

The complexity and heterogeneity of cortical circuits (Gupta et al 2000; Elston 2002; DeFelipe et al 2002; Douglas and Martin 2004; Ohki and Reid 2007) calls for guiding principles that allow us to simplify the models of the building blocks of the brain (neurons and synapses, for example), and to understand the collective behavior of a large number of interacting cells. Given the difficulty of the task, the use of simple, but appropriate, spiking models is necessary. Effective minimal models of neurons should be able to generate trains of spikes that can be compared with those observed in the brain. The IF model, pioneered by Lapicque (1907, 2007) and rediscovered by Stein (1965) (see e.g. Abbott (1999); Brunel and van Rossum (2007)), is widely used to analyze the behavior of a large number of interacting neu-

rons, but it has often been considered too simple to describe the rich dynamics of real neurons.

Results obtained in the last decade, however, have shown that the IF neuron is better than expected and quite successful at describing many of the known dynamical properties that are relevant for the collective behavior of networks of neurons. The spike response of neurons of different cortical areas can be reproduced quantitatively by IF models at the level of the first and second moment of the statistics of ISIs, as reviewed in this article, and at the level of the timing of individual spikes (Jolivet et al 2006), with a remarkable degree of accuracy.

There are at least two reasons for this success. The first one is that simplified neuron models are effective models, in the sense that they are not meant to reproduce the rich experimental phenomenology of the neuronal dynamics, but are designed to capture only the single neuron properties that are relevant for a particular collective behavior. From this perspective, the guidance provided by the mean field approach has played an important role. The second reason is that effective neuron models are entirely determined by a very small number of independent parameters. With the current experimental techniques, it is prohibitive to measure directly all the parameters that are needed for a detailed conductance-based model of the Hodgkin-Huxley type. Thus, one needs to make assumptions about the parameters that are not measured di-

rectly. These assumptions are usually based on other experimental results in which the average values across several neurons are measured. Given the high level of heterogeneity of neurons, averaging often fails to describe what happens in a particular cell (Golowasch et al 2002), whereas simplified models in which all parameters can be measured directly are more successful. Simplified models with a small number of parameters are also instrumental to study the heterogeneity of the functional properties of the cells. Models with a large number of parameters are often under-determined, i.e., they reproduce the accessible experimental data equally well with different sets of parameters. In this case, a study of the variability across neurons would be complicated by the presence of a variance component due to the ambiguity in the parameter estimation. Instead, the effective reduction of cortical firing patterns in terms of IF neurons (Sec. 5 and Table 2) is rather sensitive to small differences in the fitted cells, and additional differences can be revealed by comparing the model reductions to different types of IF neurons (Rauch et al 2003; Giugliano et al 2004; La Camera et al 2006).

There are also limitations in the use of highly simplified neuron models. More detailed models can give indications about how the neuronal properties are affected by neuromodulators and by modifications in ionic concentrations that are not easily accessible in experiments performed *in vitro* (Meunier and Segev 2002). Detailed models can also suggest how the dendritic structure and the ion dynamics can affect the statistics of the total synaptic current (see e.g. (London and Segev 2001)) (somatic current injection is admittedly a very artificial way of stimulating a neuron). On the other hand, there is unfortunately no standard model of cortical neuron. Detailed models reproduce specific phenomena and give useful indications about the underlying mechanisms, but they rarely produce predictions of new phenomena, similarly to what happens for highly simplified models. Recent discoveries of new phenomena like adaptation of fast spiking neurons on long time-scales (Reutimann et al 2004; Descalzo et al 2005; La Camera et al 2006) and the ability of prefrontal neurons to act as integrators (Winograd et al 2008) were obtained in experiments and were not predicted by the state-of-the-art detailed neuron models.

**Acknowledgements** We thank A. Rauch and H.-R. Lüscher for their many contributions to the experimental characterization of the response function of neocortical neurons. Many of the ideas and the vision behind the work described in this article were pioneered by Prof. Daniel Amit. This work is dedicated to his memory.

## References

- Abbott L (1999) Lapicque's introduction of the integrate-and-fire model neuron (1907). *Brain Res Bull* 50:303–304
- Abbott L, van Vreeswijk C (1993) Asynchronous states in networks of pulse-coupled oscillators. *Phys Rev E* 48:1483–1490
- Amit D (1995) The hebbian paradigm reintegrated: local reverberations as internal representations. *Behavioural and Brain Sciences* 18:617–657
- Amit D, Brunel N (1997a) Dynamics of a recurrent network of spiking neurons before and following learning. *Network: Computation in Neural Systems* 8:373–404
- Amit D, Brunel N (1997b) Model of global spontaneous activity and local structured (learned) delay activity during delay. *Cerebral Cortex* 7:237–252
- Amit D, Tsodyks M (1991a) Quantitative study of attractor neural network retrieving at low spike rates: I. Substrate-spikes, rates and neuronal gain. *Network* 2:259–273
- Amit D, Tsodyks M (1991b) Quantitative study of attractor neural network retrieving at low spike rates: II. Low-rate retrieval in symmetric networks. *Network* 2:275–294
- Amit D, Fusi S, Yakovlev V (1997) Paradigmatic working memory (attractor) cell in IT cortex. *Neural Computation* 9:1071–1093
- Amit DJ, Mongillo G (2003) Spike-driven synaptic dynamics generating working memory states. *Neural Computation* 15:565–596
- Arsiero M, Lüscher HR, Lundstrom B, Giugliano M (2007) The Impact of Input Fluctuations on the Frequency-Current Relationships of Layer 5 Pyramidal Neurons in the Rat Medial Prefrontal Cortex. *J Neurosci* 27:3274–3284
- Benda J, Herz A (2003) A universal model for spike-frequency adaptation. *Neural Computation* 15:2523–2564
- Braitenberg V, Schüz A (1991) *Anatomy of the cortex*. Berlin: Springer-Verlag
- Brown LD, Tony Cai T, DasGupta A (2001) Interval estimation for a binomial proportion. *Statistical Science* 16:101–133
- Brunel N (2000a) Dynamics of sparsely connected networks of excitatory and inhibitory spiking neurons. *Journal of Computational Neuroscience* 8:183–208
- Brunel N (2000b) Persistent activity and the single cell *f-I* curve in a cortical network model. *Network* 11:261–280
- Brunel N, Hakim V (1999) Fast global oscillations in networks of integrate-and-fire neurons with low firing rates. *Neural Computation* 11:1621–1671
- Brunel N, van Rossum M (2007) Lapicque's 1907 paper: from frogs to integrate-and-fire. *Biol Cybern* 97:337–339
- Brunel N, Sergi S (1998) Firing frequency of leaky integrate-and-fire neurons with synaptic currents dynamic. *J Theor Biol* 195:87–95
- Brunel N, Wang XJ (2001) Effects of neuromodulation in a cortical network model of object working memory dominated by recurrent inhibition. *Journal of Computational Neuroscience* 11:63–85
- Burkitt A (2006) A review of the integrate-and-fire neuron model: I. Homogeneous synaptic input. *Biol Cybern* 95:1–19
- Burkitt AN (2001) Balanced neurons: analysis of leaky integrate-and-fire neurons with reversal potentials. *Biol Cybern* 85:247–255
- Burkitt AN, Meffin H, Grayden DB (2003) Study of neuronal gain in a conductance-based leaky integrate-and-fire neuron model with balanced excitatory and inhibitory input. *Biol Cybern* 89:119–125
- Capocelli R, Ricciardi L (1971) Diffusion approximation and first passage time problem for a model neuron. *Kybernetik* 8:214–223
- Connors B, Gutnick M, Prince D (1982) Electrophysiological properties of neocortical neurons in vitro. *J Neurophysiol* 48:1302–1320
- Cox DR, Miller HD (1965) *The theory of stochastic processes*. New York: Chapman & Hall
- Curti E, Mongillo G, La Camera G, Amit DJ (2004) Mean-Field and capacity in realistic networks of spiking neurons storing sparsely coded random memories. *Neural Computation* 16:2597–2637
- DeFelipe J, Elston G, Fujita I, Fuster J, Harrison K, Hof P, Kawaguchi Y, Martin K, Rockland K, Thomson A, Wang S, White E, Yuste R (2002) Neocortical circuits: evolutionary aspects and specificity versus non-specificity of synaptic connections. Remarks, main conclusions and general comments and discussion. *J Neurocytol* 31:387–416
- Del Giudice P, Fusi S, Mattia M (2003) Modelling the formation of working memory with networks of integrate-and-fire neurons connected by plastic synapses. *J Physiol Paris* 97:659–681
- Descalzo V, Nowak L, Brumberg J, McCormick D, Sanchez-Vives M (2005) Slow adaptation in fast spiking neurons in visual cortex. *J Neurophysiol* 93:1111–1118

- Destexhe A, Rudolph M, Fellous JM, Sejnowski TJ (2001) Fluctuating dynamic conductances recreate in-vivo like activity in neocortical neurons. *Neuroscience* 107:13–24
- Doiron B, Lindner B, Longtin A, Maler L, Bastian J (2004) Oscillatory activity in electrosensory neurons increases with the spatial correlation of the stochastic input stimulus. *Phys Rev Lett* 93:048,101
- Douglas R, Martin K (2004) Neuronal circuits of the neocortex. *Annu Rev Neurosci* 27:419–451
- Elston G (2002) Cortical heterogeneity: implications for visual processing and polysensory integration. *J Neurocytol* 31:317–335
- Ermentrout B (1998) Linearization of f-I curves by adaptation. *Neural Computation* 10(7):1721–9
- Fleiderovich I, Friedman A, Gutnick M (1996) Slow inactivation of  $Na^+$  current and slow cumulative spike adaptation in mouse and guinea-pig neocortical neurones in slices. *J Physiol (Cambridge)* 493:83–97
- Fourcaud N, Brunel N (2002) Dynamics of the firing probability of noisy integrate-and-fire neurons. *Neural Computation* 14:2057–2110
- Fourcaud-Trocmé N, Brunel N (2005) Dynamics of the instantaneous firing rate in response to changes in input statistics. *J Comp Neurosci* 18(3):311–321
- Fourcaud-Trocmé N, Hansel H, van Vreeswijk C, Brunel N (2003) How spike generation mechanisms determine the neuronal response to fluctuating inputs. *J Neurosci* 23:11,628–11,640
- Funahashi S, Bruce C, Goldman-Rakic P (1989) Mnemonic coding of visual space in the monkey's dorsolateral prefrontal cortex. *J Neurophysiol* 61:331–349
- Fusi S, Mattia M (1999) Collective behavior of networks with linear (VLSI) integrate and fire neurons. *Neural Computation* 11:633–652
- Fusi S, Asaad W, Miller E, Wang X (2007) A neural circuit model of flexible sensorimotor mapping: learning and forgetting on multiple timescales. *Neuron* 54:319–333
- Fuster J, Jervey J (1981) Inferotemporal neurons distinguish and retain behaviorally relevant features of visual stimuli. *Science* 212:952–955
- Fuster JM (1995) *Memory in the cerebral cortex*. MIT Press
- Gabbiani F, Koch C (1998) Principles of spike train analysis. *Methods in Neuronal Modeling: From Synapses to Networks*, C Koch and I Segev, eds, 2 edition, MIT Press: Cambridge, MA pp 313–360
- Gardiner CW (1985) *Handbook of stochastic methods*. Springer
- Gershon E, Wiener M, Latham P, Richmond B (1998) Coding strategies in monkey V1 and inferior temporal cortices. *J Neurophysiol* 79:1135–1144
- Gerstner W (2000) Population dynamics of spiking neurons: fast transients, asynchronous states, and locking. *Neural Computation* 12:43–90
- Gigante G, Del Giudice P, Mattia M (2007a) Frequency-dependent response properties of adapting spiking neurons. *Math Biosci* 207:336–351
- Gigante G, Mattia M, Del Giudice P (2007b) Diverse population-bursting modes of adapting spiking neurons. *Phys Rev Lett* 98:148,101
- Giugliano M, La Camera G, Rauch A, Lüscher HR, Fusi S (2002) Non-monotonic current-to-rate response function in a novel integrate-and-fire model neuron. In JR Dorronsoro (Ed), *Proceedings of ICANN 2002, LNCS 2415*, Springer-Verlag pp 141–146
- Giugliano M, Darbon P, Arsiero M, Lüscher HR, J Streit J (2004) Single-neuron discharge properties and network activity in dissociated cultures of neocortex. *J Neurophysiol* 92:977–996
- Giugliano M, La Camera G, Fusi S, Senn W (2008) The response function of cortical neurons: theory and experiment. II. Temporal and spatial input modulations. *Biol Cybern* pp ??–??
- Golowasch J, Goldman M, Abbott L, Marder E (2002) Failure of averaging in the construction of a conductance-based neuron model. *J Neurophysiol* 87:1129–1131
- Gupta A, Wang Y, Markram H (2000) Organizing Principles for a Diversity of GABAergic Interneurons and Synapses in the Neocortex. *Science* 287:273–278
- Gutkin B, Ermentrout G (1997) Dynamics of membrane excitability determine interspike interval variability: a link between spike generation mechanisms and cortical spike train statistics. *Neural Computation* 10(5):1047–1065
- Hanson FB, Tuckwell HC (1983) Diffusion approximation for neural activity including synaptic reversal potentials. *J Theor Neurobiol* 2:127–153
- Higgs M, Slee S, Spain W (2006) Diversity of gain modulation by noise in neocortical neurons: regulation by the slow afterhyperpolarization conductance. *J Neurosci* 26:8787–8799
- Holden AV (1976) *Models of stochastic activity of neurons*. Springer Verlag, New York
- Holt G, Softky W, Koch C, Douglas R (1996) Comparison of discharge variability in vitro and in vivo in cat cortex neurons. *J Neurophysiol* 75(5):1806–1814
- Johannesma PIM (1968) Diffusion models for the stochastic activity of neurons. In *Neural Networks*, edited by ER Caianiello, Springer, Berlin, pp 116–144
- Jolivet R, Lewis T, Gerstner W (2004) Generalized integrate-and-fire models of neuronal activity approximate spike trains of a detailed model to a high degree of accuracy. *J Neurophysiol* 92:959–976
- Jolivet R, Rauch A, Lüscher H, Gerstner W (2006) Predicting spike timing of neocortical pyramidal neurons by simple threshold models. *J Comput Neurosci* 21:35–49
- Jolivet R, Kobayashi R, Rauch A, Naud R, Shinomoto S, Gerstner W (2008) A benchmark test for a quantitative assessment of simple neuron models. *J Neurosci Methods* 169:417–424
- Knight BW (1972a) Dynamics of encoding of a populations of neurons. *The Journal of General Physiology* 59:734–736
- Knight BW (1972b) The relationship between the firing rate of a single neuron and the level of activity in a network of neurons. Experimental evidence for resonance enhancement in the population response. *The Journal of General Physiology* 59:767
- Koch K, Fuster J (1989) Unit activity in monkey parietal cortex related to haptic perception and temporary memory. *Exp Brain Res* 76:292–306
- Kostal L, Lánský P, Rospars J (2007) Neuronal coding and spiking randomness. *Eur J Neurosci* 26:2693–2701
- Kumar A, Rotter S, Aertsen A (2008a) Conditions for propagating synchronous spiking and asynchronous firing rates in a cortical network model. *J Neurosci* 28:5268–5280
- Kumar A, Schrader S, Aertsen A, Rotter S (2008b) The high-conductance state of cortical networks. *Neural Comput* 20:1–43
- La Camera G (1999) Learning overlapping stimuli in a recurrent network of spiking neurons (in Italian). Università di Roma "La Sapienza", Roma, Italy
- La Camera G, Rauch A, Senn W, Lüscher HR, Fusi S (2002) Firing rate adaptation without losing sensitivity to input fluctuations. In JR Dorronsoro (Ed), *Proceedings of ICANN 2002, LNCS 2415*, Springer-Verlag pp 180–185
- La Camera G, Rauch A, Senn W, Lüscher HR, Fusi S (2004a) Minimal models of adapted neuronal response to *in vivo*-like input currents. *Neural Computation* 16:2101–2124
- La Camera G, Senn W, Fusi S (2004b) Comparison between networks of conductance- and current-driven neurons: stationary spike rates and subthreshold depolarization. *Neurocomputing* 58-60C:253–258
- La Camera G, Rauch A, Thurbon D, Lüscher HR, Senn W, Fusi S (2006) Multiple time scales of temporal response in pyramidal and fast spiking cortical neurons. *J Neurophysiol* 96:3448–3464
- Lánský P, Lánská V (1987) Diffusion approximation of the neuronal model with synaptic reversal potentials. *Biol Cybern* 56:19–26
- Lánský P, Sato S (1999) The stochastic diffusion models of nerve membrane depolarization and interspike interval generation. *Journal of the Peripheral Nervous System* 4:27–42
- Lapicque L (1907) Recherches quantitatives sur l'excitation électrique des nerfs traitée comme une polarisation. *J Physiol Pathol Gen* 9:620–635
- Lapicque L (2007) Quantitative investigations of electrical nerve excitation treated as polarization. 1907. *Biol Cybern* 97:341–349

- Larkum M, Senn W, Lüscher H (2004) Top-down dendritic input increases the gain of layer 5 pyramidal neurons. *Cereb Cortex* 14:1059–1070
- Larkum ME, Zhu JJ, Sakmann B (1999) A new cellular mechanism for coupling inputs arriving at different cortical layers. *Nature* 398:338–341
- Lee D, Port N, Kruse W, Georgopoulos A (1998) Variability and Correlated Noise in the Discharge of Neurons in Motor and Parietal Areas of the Primate Cortex. *J Neurosci* 18(3):1161–1170
- Lerchner A, Ursta C, Hertz J, Ahmadi M, Ruffiot P, Enemark S (2006) Response variability in balanced cortical networks. *Neural Comput* 18(3):634–659
- Lindner B, Schimansky-Geier L, Longtin A (2002) Maximizing spike train coherence or incoherence in the leaky integrate-and-fire model. *Phys Rev E Stat Nonlin Soft Matter Phys* 66:031,916
- Liu YH, Wang XJ (2001) Spike-frequency adaptation of a generalized leaky integrate-and-fire model neuron. *Journal of Computational Neuroscience* 10:25–45
- London M, Segev I (2001) Synaptic scaling in vitro and in vivo. *Nat Neurosci* 4:853–855
- Lowen S, Teich M (1992) Auditory-nerve action potentials form a non-renewal point process over short as well as long time scales. *J Acoust Soc Am* 92(2 Pt 1):803–806
- Mascaro M, Amit D (1999) Effective neural response function for collective population states. *Network: Computation in Neural Systems* 10:351–373
- Mattia M, Del Giudice P (2002) Population dynamics of interacting spiking neurons. *Phys Rev E* 66:051,917
- McCormick DA, Connors BW, Lighthall JW, Prince D (1985) Comparative electrophysiology of pyramidal and sparsely stellate neurons of the neocortex. *J Neurophysiol* 54:782–806
- Meunier C, Segev I (2002) Playing the devil's advocate: is the Hodgkin-Huxley model useful? *Trends Neurosci* 25:558–563
- Meyer PL (1965) *Introductory Probability and Statistical Applications*. Addison Welsley, Reading Mass., page 287
- Mezard M, Parisi G, Virasoro MA (1987) *Spin glass theory and beyond*. Singapore: World Scientific
- Miyashita Y (1988) Neural correlate of visual associative long-term memory in the primate temporal cortex. *Nature* 335:817–820
- Miyashita Y, Chang H (1988) Neural correlate of pictorial short-term memory in the primate temporal cortex. *Nature* 331:68–70
- Mongillo G, Barak O, Tsodyks M (2008) Synaptic theory of working memory. *Science* 319:1543–1546
- Moreno R, de la Rocha J, Renart A, Parga N (2002) Response of spiking neurons to correlated inputs. *Physical Review Letters* 89:288,101
- Moreno-Bote R, Parga N (2004) Role of synaptic filtering on the firing response of simple model neurons. *Phys Rev Lett* 92:028,102
- Moreno-Bote R, Parga N (2005) Membrane potential and response properties of populations of cortical neurons in the high conductance state. *Phys Rev Lett* 94:088,103
- Moreno-Bote R, Renart A, Parga N (2008) Theory of input spike auto- and cross-correlations and their effect on the response of spiking neurons. *Neural Comput* 20:1651–1705
- Muller E, Buesing L, Schemmel J, Meier K (2007) Spike-frequency adapting neural ensembles: beyond mean adaptation and renewal theories. *Neural Comput* 19:2958–3010
- Noda H, Adey W (1970) Firing variability in cat association cortex during sleep and wakefulness. *Brain Res* 18:513–526
- Nykamp D, Tranchina D (2000) A population density approach that facilitates large-scale modeling of neural networks: analysis and an application to orientation tuning. *J Comput Neurosci* 8:19–50
- Ohki K, Reid R (2007) Specificity and randomness in the visual cortex. *Curr Opin Neurobiol* 17:401–407
- Oram M, Wiener M, Lestienne R, Richmond B (1999) Stochastic nature of precisely timed spike patterns in visual system neural responses. *J Neurophysiol* 81:3021–3033
- Powers R, Sawczuk A, Musick J, Binder M (1999) Multiple mechanisms of spike-frequency adaptation in motoneurons. *J Physiol (Paris)* 93:101–114
- Rauch A, La Camera G, Lüscher HR, Senn W, Fusi S (2003) Neocortical cells respond as integrate-and-fire neurons to *in vivo*-like input currents. *J Neurophysiol* 90:1598–1612
- Reich D, Victor J, Knight B, Ozaki T, Kaplan A (1997) Response variability and timing precision of neuronal spike trains in vivo. *J Neurophysiol* 77:2836–2841
- Renart A, Brunel N, Wang XJ (2003) Mean-field theory of recurrent cortical networks: from irregularly spiking neurons to working memory. In: *Computational Neuroscience: A Comprehensive Approach* J Feng (Ed), CRC Press, Boca Raton
- Reutimann J, Yakovlev V, Fusi S, Senn W (2004) Climbing neuronal activity as an event-based cortical representation of time. *J Neurosci* 24:3295–3303
- Richardson MJE (2004) The effects of synaptic conductance on the voltage distribution and firing rate of spiking neurons. *Phys Rev E* 69:051,918
- Richardson MJE (2007) Firing-rate response of linear and nonlinear integrate-and-fire neurons to modulated current-based and conductance-based synaptic drive. *Phys Rev E* 76:021,919
- Richardson MJE, Gerstner W (2005) Synaptic shot noise and conductance fluctuations affect the membrane voltage with equal significance. *Neural Computation* 17:923–947
- Rigotti M, Ben Dayan Rubin D, Wang X, Fusi S (2008) Internal representation of task rules by recurrent dynamics: the importance of the diversity of neural responses. Submitted
- Rolls ET, Deco G (2001) *The Computational Neuroscience of Vision*. Oxford University Press
- van Rossum M, Turrigiano G, Nelson S (2002) Fast propagation of firing rates through layered networks of noisy neurons. *J Neurosci* 22:1956–1966
- Sah P (1996)  $Ca^{2+}$ -activated  $K^{+}$  currents in neurons: types, physiological roles and modulation. *Trends Neurosci* 19:150–154
- Sakai Y, Funahashi S, Shinomoto S (1999) Temporally correlated inputs to leaky integrate-and-fire models can reproduce spiking statistics of cortical neurons. *Neural Netw* 12(7-8):1181–1190
- Salinas E, Sejnowski TJ (2001) Gain modulation in the central nervous system: where behavior, neurophysiology and computation meet. *The Neuroscientist* 7:430–440
- Salinas E, Sejnowski TJ (2002) Integrate-and-fire neurons driven by correlated stochastic input. *Neural Computation* 14:2111–2155
- Salinas E, Thier P (2000) Gain modulation: A major computational principle of the central nervous system. *Neuron* 27:15–21
- Sanchez-Vives M, Nowak L, McCormick D (2000) Cellular mechanisms of long-lasting adaptation in visual cortical neurons *in vitro*. *J Neurosci* 20:4286–4299
- Sawczuk A, Powers R, Binder M (1997) Contribution of outward currents to spike frequency adaptation in hypoglossal motoneurons of the rat. *Journal of Physiology* 78:2246–2253
- Shadlen M, Newsome W (1998) The variable discharge of cortical neurons: implications for connectivity, computation and information coding. *J Neurosci* 18:3870–3896
- Shinomoto S, Shima K, Tanji J (2003) Differences in spiking patterns among cortical neurons. *Neural Computation* 15(12):2823–2842
- Stein RB (1965) A theoretical analysis of neuronal variability. *Biophys J* 5:173–194
- Svirskis G, Rinzel J (2000) Influence of temporal correlation of synaptic input on the rate and variability of firing in neurons. *Biophys J* 5:629–637
- Thurley K, Senn W, Lüscher H (2008) Dopamine increases the gain of the input-output response of rat prefrontal pyramidal neurons. *J Neurophysiol* 99(6):2985–97
- Treves A (1993) Mean field analysis of neuronal spike dynamics. *NETWORK* 4:259–284
- Troyer T, Miller K (1997) Physiological gain leads to high ISI variability in a simple model of a cortical regular spiking cell. *Neural Computation* 9:971–983
- Tsodyks M, Markram H (1997) The neural code between neocortical pyramidal neurons depends on neurotransmitter release probability. *PNAS* 94:719–723

- 
- 1  
2  
3  
4  
5  
6 Tsodyks M, Pawelzik K, Markram H (1998) Neural networks with dynamic synapses. *Neural Computation* 10:821–835
- 7  
8 Tuckwell HC (1988) *Introduction to theoretical neurobiology*. Cambridge: Cambridge University Press (MA)
- 9  
10 Ulanovsky N, Las L, Farkas D, Nelken I (2004) Multiple time scales of adaptation in auditory cortex neurons. *J Neurosci* 24:10,440–10,453
- 11  
12 Victor J (2005) Spike train metrics. *Curr Opin Neurobiol* 15(5):585–592
- 13  
14 Vogels T, Abbott L (2005) Signal propagation and logic gating in networks of integrate-and-fire neurons. *J Neurosci* 25:10,786–10,795
- 15  
16 van Vreeswijk C, Sompolinsky H (1996) Chaos in Neuronal Networks with Balanced Excitatory and Inhibitory Activity. *Science* 274:1724–1726
- 17  
18 Wang XJ (1998) Calcium coding and adaptive temporal computation in cortical pyramidal neurons. *J Neurophysiol* 79:1549–66
- 19  
20 Wang XJ (1999) Synaptic basis of cortical persistent activity: the importance of NMDA receptors to working memory. *J Neurosci* 19(21):9587–9603
- 21  
22 Wang XJ (2001) Synaptic reverberation underlying mnemonic persistent activity. *Trends in Neurosciences* 24(8):455–463
- 23  
24 Wang XJ (2002) Probabilistic decision making by slow reverberation in cortical circuits. *Neuron* 36:955–968
- 25  
26 Wiener MC, Oram MW, Liu Z, Richmond BJ (2001) Consistency of encoding in monkey visual cortex. *J Neurosci* 21(20):8210–8221
- 27  
28 Wilbur W, Rinzel J (1983) A theoretical basis for large coefficient of variation and bimodality in neuronal interspike interval distribution. *J Theor Biol* 105:345–368
- 29  
30 Wilson F, Scialidhe S, Goldman-Rakic P (1993) Dissociation of object and spatial processing domains in primate prefrontal cortex. *Science* 260:1955–1958
- 31  
32 Winograd M, Destexhe A, Sanchez-Vives M (2008) Hyperpolarization-activated graded persistent activity in the prefrontal cortex. *Proc Natl Acad Sci USA* 105:7298–7303
- 33  
34 Wong KF, Wang XJ (2006) A recurrent network mechanism of time integration in perceptual decisions. *J Neurosci* 26:1314–1328
- 35  
36 Yakovlev V, Fusi S, Berman E, Zohary E (1998) Inter-trial neuronal activity in infero-temporal cortex: a putative vehicle to generate long term associations. *Nature Neuroscience* 1:310–317
- 37  
38  
39  
40  
41  
42  
43  
44  
45  
46  
47  
48  
49  
50  
51  
52  
53  
54  
55  
56  
57  
58  
59  
60  
61  
62  
63  
64  
65